complementing our data demonstrating the genetic concordance of both immunophenotypic subpopulations in patient 2279.

In summary, although we used complex genomic analyses, we did not identify any genetic aberrations that were specifically present in only 1 of the immunophenotypically distinct subpopulations in either of the 2 patients investigated upon the diagnosis of BLL. Although we cannot exclude that such aberrations triggering the immunophenotypic lineage split (or contributing to it) do exist in certain BLLs, this does not appear to be a general mechanism, at least in T/myeloid BLL. Conversely, mutational analysis of *WT1* in patient 2279 suggests that lineage plasticity is inherent to the vast majority of leukemic blasts, which alter their transcriptional programs and differentiate into different lineages in a stochastic manner. Our results shed new light on BLL: not only can all immunophenotypically heterogeneous leukemic populations be derived from an identical founder cell, but multiple leukemic cells possess the potential to differentiate into very distinct cell types. Further studies with large cohorts are needed to elucidate whether this lineage plasticity in BLL associates with certain specific genetic and/or epigenetic backgrounds.

The online version of this article contains a data supplement.

Acknowledgments: This work was supported by grants from the Czech Ministries of Health (AZV 15-30626A and AZV 15-28525A), and Education (NPU I LO1604), and by the Project for Conceptual Development of Research Organization 00064203 (University Hospital Motol, Prague, Czech Republic).

Contribution: M.K. and M.Z. performed the genetic analyses; E.M. and O.H. performed the immunophenotyping and cell sorting; A.M., J. Stuchly, and K.F. performed the bioinformatic analyses; M.K. and M.Z. performed the postbioinformatic analyses; M.K., M.Z., J. Starkova, J. Stary, J.Z., O.H., and J.T. integrated and interpreted the results; O.H., J.T., and M.Z. designed the study; M.Z. led the study and wrote the manuscript; and all authors revised and approved the manuscript.

Conflict-of-interest disclosure: The authors declare no competing financial interests.

Correspondence: Jan Trka, Childhood Leukaemia Investigation Prague, Department of Paediatric Haematology and Oncology, Second Faculty of Medicine, Charles University, V Uvalu 84, 150 06 Prague, Czech Republic; e-mail: jan.trka@lfmotol.cuni.cz.

References

1. Hrusak O, Luks A, Janotova I, et al. Acute Leukemias of Ambiguous Lineage; Study on 247 Pediatric Patients [abstract]. *Blood.* 2015;126(23). Abstract 252.
2. Jan M, Majeti R. Clonal evolution of acute leukemia genomes. *Oncogene.* 2013; 32(2):135-140.
3. Tosello V, Mansour MR, Barnes K, et al. WT1 mutations in T-ALL. *Blood.* 2009; 114(5):1038-1045.
4. Zhang J, Ding L, Holmfeldt L, et al. The genetic basis of early T-cell precursor acute lymphoblastic leukaemia. *Nature.* 2012;481(7380):157-163.
5. Kontro M, Kuusanmäki H, Eldfors S, et al. Novel activating STAT5B mutations as putative drivers of T-cell acute lymphoblastic leukemia. *Leukemia.* 2014;28(8):1738-1742.
6. Liu Y, Easton J, Shao Y, et al. The Genomic Landscape of Childhood T-Lineage Acute Lymphoblastic Leukemia [abstract]. *Blood.* 2015;126(23). Abstract 691.
7. Gremer L, Merbitz-Zahradnik T, Dvorsky R, et al. Germline KRAS mutations cause aberrant biochemical and physical properties leading to developmental disorders. *Hum Mutat.* 2011;32(1):33-43.
8. Mullighan CG, Goorha S, Radtke I, et al. Genome-wide analysis of genetic alterations in acute lymphoblastic leukaemia. *Nature.* 2007;446(7137):758-764.
9. Jones CL, Bhatla T, Blum R, et al. Loss of TBL1XR1 disrupts glucocorticoid receptor recruitment to chromatin and results in glucocorticoid resistance in a B-lymphoblastic leukemia model. *J Biol Chem.* 2014;289(30):20502-20515.

DOI 10.1182/blood-2016-07-725861

To the editor:

Coexistence of gain-of-function *JAK2* germ line mutations with *JAK2*^{V617F} in polycythemia vera

Lucie Lanikova,[1-3] Olga Babosova,[3] Sabina Swierczek,[1,2] Linghua Wang,[4] David A. Wheeler,[4] Vladimir Divoky,[5,6] Vladimir Korinek,[3] and Josef T. Prchal[1,2,7]

[1]Division of Hematology, University of Utah School of Medicine, Salt Lake City, UT; [2]George E. Wahlen Department of Veterans Affairs Medical Center, Salt Lake City, UT; [3]Department of Cell and Developmental Biology, Institute of Molecular Genetics, Academy of Sciences of the Czech Republic, Prague, Czech Republic; [4]Human Genome Sequencing Center, Baylor College of Medicine, Houston, TX; [5]Department of Biology, Faculty of Medicine and Dentistry, Palacky University, Olomouc, Czech Republic; [6]Department of Biology, Faculty of Medicine, Masaryk University, Brno, Czech Republic; and [7]Department of Pathophysiology and 1st Department of Medicine, 1st Faculty of Medicine, Charles University, Prague, Czech Republic

Philadelphia chromosome–negative myeloproliferative neoplasms (MPNs) can be viewed as clonal premalignant disorders that precede development of acute leukemia wherein the order of mutation acquisition, together with environmental insults such as inflammation, matters. MPN disease-defining somatic mutations are in Janus kinase 2 (*JAK2*), calreticulin (*CALR*), and myeloproliferative leukemia virus oncogene (*MPL*; a gene encoding thrombopoietin receptor) genes. Several studies have revealed other somatic mutations affecting intracellular signaling of hematopoietic stem cells in MPNs, but these are considered as phenotype-modifying, not disease-initiating, mutations (reviewed by Tefferi and Pardanani[1]), such as Tet methylcytosine dioxygenase 2 (*TET2*) mutations, which may precede or follow acquisition of *JAK2*^{V617F}.[2-4] However, the order of *TET2* mutation occurrence alters the transcriptional program in hematopoietic stem cells and patients' clinical outcome.[5]

In polycythemia vera (PV), the *JAK2*^{V617F} mutation is present in the vast majority of patients, yet is not always the disease-initiating mutation and constitutes only part of the clone.[6,7] We reported in 2014 the mutational landscape of 31 *JAK2*^{V617F}-positive PV patients[4,8] and identified 2 patients with an acquired polycythemia phenotype carrying *JAK2* variants at conserved residues of *JAK2*: first (T108A) in the 4-point, ezrin, radixin, moesin (FERM) domain, and the other (L393V) in 7 amino acids upstream of the Src homology 2 (SH2) domain (Figure 1A-C). Both mutations were verified by Sanger sequencing in DNA isolated from patients' granulocytes, and then proven to be heterozygous germ line mutations by their presence in T cells and nail DNA. Protein prediction algorithms (SIFT,[9] AGVGD,[10] and PolyPhen[11]) considered both variants as tolerated, benign, and light, respectively, but both variants were predicted to be damaging by MutationTaster[12] and possibly damaging by LoFtool.

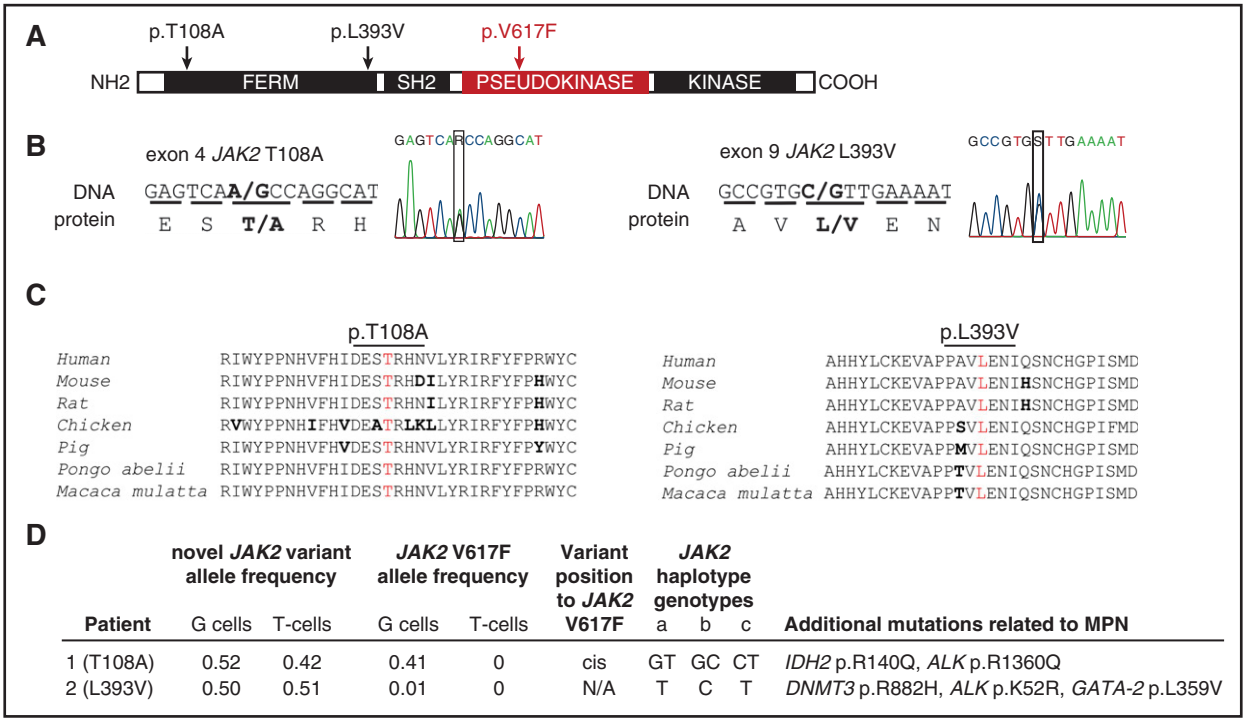

D

Patient	novel *JAK2* variant allele frequency G cells	T-cells	*JAK2* V617F allele frequency G cells	T-cells	Variant position to *JAK2* V617F	*JAK2* haplotype genotypes a	b	c	Additional mutations related to MPN
1 (T108A)	0.52	0.42	0.41	0	cis	GT	GC	CT	*IDH2* p.R140Q, *ALK* p.R1360Q
2 (L393V)	0.50	0.51	0.01	0	N/A	T	C	T	*DNMT3* p.R882H, *ALK* p.K52R, *GATA-2* p.L359V

Figure 1. Clinical and molecular features of 2 PV patients with germ line *JAK2* mutations, T108A and L393V. (A) The schematic structure of the JAK2 domains with depicted locations of T108A and L393V mutations and V617F. (B) Sequencing analysis of germ line *JAK2* mutations, causing an amino acid substitutions at codon 108 (threonine to alanine, p.T108A, c.A322G, novel mutation) and codon 393 (leucine to valine, p.L393V, c.C1177G, rs2230723; G allele presented in 1% of the population). (C) Alignment of amino acid sequences of JAK2 residues 93 to 125 and 379 to 407 (human JAK2 nomenclature) from different species shows highly conserved pattern. Conserved residues are colored in black, differences are in bold, and the residues at which the mutation occurs are in red. (D) The mutational screening was determined by whole exome sequencing (details published elsewhere[4,8]). G cells, granulocytes; T cells, $CD3^+$ T lymphocytes. The chromosomal position of new mutation toward V617F was determined by cDNA cloning, followed by Sanger sequencing. *JAK2* GGCC haplotype represents a set of single nucleotide polymorphisms (SNPs) that are associated with a predisposition to MPN.[24] *JAK2* GGCC haplotype was determined using polymerase chain reaction and TaqMan SNP assay on demand: (a) rs3780367, C_27515396_10, **G**/T, intron 10; (b) rs10974944, C_31941696_10, **G**/C, intron 12; (c) rs12343867, C_319416 89_10, **C**/T, intron 14. Several other acquired mutations that may have contributed to their MPN pathogenesis and clinical course were found in both patients. The allele frequencies of these mutations in patients' granulocytes were as follows: *IDH2* p.R140Q, 0.43; *ALK* p.R1360Q, 0.14; *DNMT3* p.R882H, 0.31; *ALK* p.K52R, 0.13; *GATA-2* p.L359V, 0.19 (sequencing, annotation, and validation details published elsewhere[4,8]).

Nevertheless, the functional significance of these germ line *JAK2* variants and their putative predisposition to PV are not known.

The first patient ($JAK2^{T108A}$) had a $JAK2^{V617F}$ allele burden of 41% in granulocytes. He initially presented 13 months prior to our encounter with hemoglobin 19.4 g%, thrombocytosis of 535×10^9/L, mild leukocytosis (11.3×10^9/L), and recent history of pulmonary embolism. Detailed family history was not available, but there was an undocumented history of increased hematocrit in maternal uncle. Subsequent therapy with hydroxyurea normalized his blood counts. He moved to a different state, and several months later, he developed bone pain, prostration, thrombocytopenia, and transfusion-requiring anemia and died with fulminant blast transformation. The second patient ($JAK2^{L393V}$) was ethnic Japanese who had a preceding 12-year history of initially isolated thrombocytosis followed within an ensuing year also by erythrocytosis. He had a history of coronary thromboses. He achieved normalization of blood counts by hydroxyurea therapy. At the time of the study, he had very low $JAK2^{V617F}$ allele burden at 1% (confirmed by sensitive quantitative $JAK2^{V617F}$ assay[6]). A year later, he became anemic, and hydroxyurea therapy was stopped. His marrow showed ~10% of blasts. In the ensuing 2 years, he developed progressive pancytopenia with increasing blasts; he then refused supporting therapy, at which time he developed leukocytosis and peripheral blood blast count exceeding 75%, refused further supportive therapy, and died. Their other mutations detected at the time of the study that may have contributed to their PV phenotype are depicted in Figure 1D.[4]

We first analyzed individual burst-forming unit erythroid colonies (BFU-Es) for erythropoietin (EPO)–independent growth (EECs) from the patient with $JAK2^{L393V}$. All individually genotyped colonies had wild-type (wt) and $JAK2^{L393V}$ alleles in similar proportions, and only 1 EEC (1/16) had an equal proportion of $JAK2^{V617F}$ and wt alleles (heterozygous). Material from the $JAK2^{T108A}$ patient was not available for BFU-E analyses; however, we cloned and sequenced his complementary DNA (cDNA) from his granulocytes and found that $JAK2^{T108A}$ and $JAK2^{V617F}$ were *cis*. In the patient with the $JAK2^{L393V}$ mutation, a paucity of material and low allelic burden of $JAK2^{V617F}$ precluded determination of a $JAK2^{L393V/V617F}$ configuration.

Unfortunately, in silico modeling of potential interactions of JAK2 germ line variants cannot be obtained because the structure of the JAK2 FERM domain is not yet available, whereas in the structure of the TYK2 FERM domain, these residues are exposed and do not appear to interact with other residues that lack the kinase and pseudokinase domains or with partners of other receptor subunits.[13] Interestingly, our JAK2 variants contain precise residues of TYK2 at the 108 (Ala) and 393 (Val) positions, suggesting that, in themselves, they are compatible with functional JAK kinases. TYK2 functions in heteromeric receptor complexes, whereas JAK2 functions in homodimeric receptor complexes, and it is possible that these exposed residues play a role in limiting JAK2 self-activation.

In order to determine the functional consequences of *JAK2* germ line mutations on the PV phenotype, we generated stably transfected Ba/F3 cell lines expressing erythropoietin receptor (EPOR) and JAK2

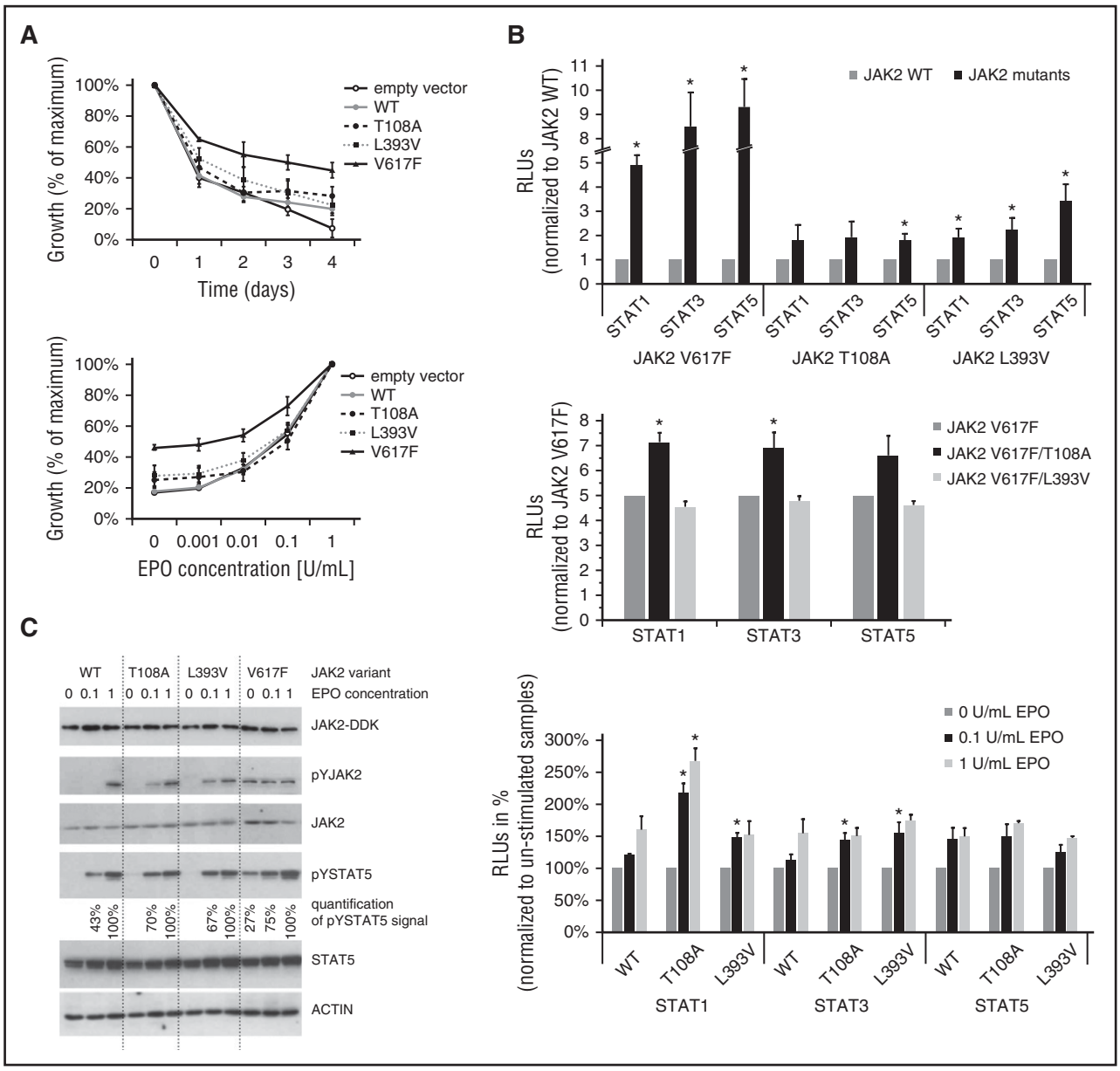

Figure 2. Functional modeling and characterization of 2 *JAK2* germ line mutations, T108A and L393V. The methods are described in the supplemental Methods (available on the *Blood* Web site). The Ba/F3-EPOR cells (5×10^5 cells per sample) were nucleofected with 2 μg pCMV6-AC-IRES-GFP-Puro "empty" vector or the construct encoding wt or mutated forms of JAK2 kinase (as indicated) using AMAXA II device (program X_001). Transfected cells were selected with 2 μg/mL puromycin for 2 weeks. (A) Proliferation of cells in the absence of EPO was quantified by CellTitre-Blue reagent (Promega, Madison, WI) and Perkin-Elmer Envision analyzer (top). Data are expressed as a percentage of maximum value at starting point (day 0). Results are shown as the mean (± standard deviation [SD]) of 3 independent experiments performed in triplicate. Proliferation of cells in increased concentrations of EPO (0, 0.001, 0.01, 0.1, and 1 U/mL) were quantified by CellTitre-Blue reagent (Promega) and Perkin-Elmer Envision analyzer (bottom). Data are expressed as a percentage of maximum value (EPO 1 U/mL). Results are shown as the mean (± SD) of 3 independent experiments performed in triplicate. (B) Luciferase reporter assay. STAT-dependent transcriptional activity induced by JAK2 variants was measured using firefly luciferase STAT reporter (pGl4.26/GRR4.CZ) in HCT116 cells. Reporter plasmid was constructed with STAT responsive elements,[25] when single-stranded oligos were annealed, ligated, and cloned to pGl4.26 reporter backbone. The ratios of constructs in the transfection mixtures (ie, plasmids producing JAK2, EPOR, STATs, the luciferase reporter, and the Renilla control vector) were determined by titration experiments. Luminescence was measured 48 hours after transfection, and Renilla counts were used as internal control (top). Shown are averages ± standard error of the mean (SEM) of 5 independent experiments performed in duplicate. Two-tailed Student *t* test: $^*P > .05$. JAK2 double mutants were created by site directed mutagenesis of the pCMV6-JAK2V617F-IRES-GFP-Puro expression plasmid (middle). Luminescence was measured 48 hours after transfection, and Renilla counts were used as internal control. Shown are averages ± SEM of 3 independent experiments performed in duplicate. Two-tailed Student *t* test: $^*P > .05$. Luminescence was measured 24 hours after EPO stimulation (48 hours after transfection), and Renilla counts were used as internal control (bottom). Shown are averages ± SEM of 3 independent experiments performed in duplicate. Two-tailed Student *t* test: $^*P > .05$. (C) Protein assay. The level of human JAK2 protein in stably transfected Ba/F3-EPOR cell-lines is equal, as indicated by western blot using anti-DDK antibody (Cell Signaling Technology). Ba/F3-EPOR cells expressing different JAK2 wt and mutant variants were cytokine starved for 6 hours and then shortly stimulated. Western blots were performed with rabbit JAK2, pYJAK2 (Tyr 1007/1008), pYSTAT5 (Tyr 694), and STAT5 (Cell Signaling Technology) antibodies, and actin (Sigma-Aldrich, St. Louis, MO) was used as a loading control. JAK2 V617F samples for JAK2/pJAK2 were run on separate gel than the rest of the samples. Signal for pYSTAT5 was quantified using densitometric analysis by ImageJ software.

variants (T108A, L393V, V617F, and wt). Cells expressing $JAK2^{V617F}$ were EPO independent, and their viability was significantly increased in comparison with $JAK2^{WT}$-expressing cells, which did not grow in the absence of EPO and proliferated less at various EPO concentrations. The 2 interrogated *JAK2* mutants were dependent on EPO but were hypersensitive (Figure 2A). Response to a JAK2 inhibitor

(LY2784544)[14] was similar for both germ line and wt JAK2 variants at different concentrations of LY2784544 after 72 hours of exposure (data not shown).

We evaluated signal transduction of JAK2 mutant and wt kinases, as measured by STAT activation, using dual luciferase assays with STAT responsive elements reporter plasmid. STAT activation was markedly increased without EPO for $JAK2^{V617F}$ and less so, but still more, compared with wt in both germ line variants ($P < .05$; Figure 2B, top). Using double mutants in the luciferase assay, only *cis* configuration of T108A/V617F increased the STAT activation above $JAK2^{V617F}$ signal ($P < .05$; Figure 2B, middle). The L393V mutation does not seem to synergize in augmenting V617F signaling, which is consistent with only 1% V617F allele burden in the patients' granulocytes. It is possible that $JAK2^{L393V}$ variant synergizes with other acquired mutations with higher allele frequency in this patient (Figure 1D), but without further study, the existence of such cooperation of these mutations should be interpreted with caution. We then stimulated cells with different EPO concentrations (0,1, and 1 U/mL, EPO added 24 hours after transfection) and determined STATs activation. Increased STAT activation by EPO was significant only at low concentrations of EPO ($P < .05$; Figure 2B, bottom) for both germ line mutants, whereas no further increase of STAT activation was observed in already markedly hyperactive $JAK2^{V617F}$-transfected cells after addition of EPO (data not shown).

We also investigated JAK/STAT signaling in stably transfected Ba/F3-EPOR cell lines. Cells were cytokine starved for 6 hours and then stimulated with an increased concentration of EPO for 15 minutes. Similar levels of human JAK2 protein in all cell lines were verified by western blot using anti-DDK antibody (Cell Signaling Technology, Danvers, MA). Constitutive activation of the STAT5 pathway was obvious in $JAK2^{V617F}$-expressing cells in the absence of EPO. We repeatedly observed stronger phosphorylation of JAK2 and STAT5 at low concentrations of EPO in both mutant variants (T108A, L393V) in comparison with $JAK2^{WT}$ cell line (Figure 2C).

Because *JAK2* germ line mutations in MPNs were identified at the same time as oncogenic $JAK2^{V617F}$,[15] their impact on JAK2 kinase activity and effect on disease initiation or progression have not been fully evaluated. Several germ line mutations in addition to the somatic $JAK2^{V617F}$ mutation in JAK2 pseudo-kinase domains can induce MPN phenotype (eg, R564Q[16] and V625F[17]) or isolated thrombocytosis (V617I[18]) and erythrocytosis (E846D and R1063H),[19] but our data also suggest that germ line mutations outside the core regulatory domain can alter the EPO-sensing properties of cells and therefore may provide proliferation advantage. Because the JAK2 FERM domain is required for EPOR association and consequent relief of inhibitory conformation of the kinase domain that leads to JAK2 activation,[20,21] the molecular basis of this activation remains to be elucidated.

To our knowledge, this is the first description of an association of gain-of-function germ line *JAK2* mutations coexisting with $JAK2^{V617F}$ in subjects with PV phenotypes. Interestingly, these propositi had documented normal blood counts for decades prior to their PV diagnosis. However, after developing the PV phenotype, both eventually died of acute myeloid leukemia (AML) or myelodysplastic syndrome transforming within months to AML. Whether these germ line mutations increase the probability of acquiring PV is suggestive; both mutations were found in analysis of 31 unrelated PV subjects (statistically unlikely to be a random occurrence), and, in 1 subject, $JAK2^{T108A}$ and $JAK2^{V617F}$ were in *cis*. In addition, the L393V mutation was found with increased frequency among diffuse large B-cell tumors,[22] and T108A has been reported in an adenocarcinoma cell line,[23] further supporting their potential to predispose to malignancy.

In conclusion, we hypothesize that *JAK2* germ line mutations may represent a mechanism that may precede acquisition of $JAK2^{V617F}$ lesion during the evolution of PV phenotype and may contribute to further genomic alterations in PV clone and perhaps even leukemic transformation.

The online version of this article contains a data supplement.

Acknowledgments: The authors thank Stefan Constantinescu and Emilie Leroy for their insights into the JAK2 protein interactions and valuable input to this manuscript. This work was supported by research funding from the Czech Science Foundation, project GACR 15-18046Y; the Ministry of Education, Youth and Sports, Czech Republic, Program NPU I, Project LO1419 (L.L., O.B., and V.K.); and Myeloproliferative Disorders Research Consortium (National Cancer Institute, National Institutes of Health [grant P01CA108671] [J.T.P.]).

Contribution: L.L., V.D., and J.T.P. designed and conceived the project and the experiments; L.L., O.B., and S.S. performed the experiments; D.A.W., L.W., and J.T.P. performed and analyzed the whole exome sequencing; L.L., V.D., and J.T.P. wrote the manuscript; and S.S., D.A.W., L.W., and V.K. critically reviewed the manuscript.

Conflict-of-interest disclosure: The authors declare no competing financial interests.

Correspondence: Josef T. Prchal, Division of Hematology, 30 N 1900 E, 5C402 SOM, University of Utah, Salt Lake City, UT 84132; e-mail: josef.prchal@hsc.utah.edu.

References

1. Tefferi A, Pardanani A. Myeloproliferative neoplasms: a contemporary review. *JAMA Oncol.* 2015;1(1):97-105.
2. Delhommeau F, Dupont S, Della Valle V, et al. Mutation in TET2 in myeloid cancers. *N Engl J Med.* 2009;360(22):2289-2301.
3. Schaub FX, Looser R, Li S, et al. Clonal analysis of TET2 and JAK2 mutations suggests that TET2 can be a late event in the progression of myeloproliferative neoplasms. *Blood.* 2010;115(10):2003-2007.
4. Wang L, Swierczek SI, Drummond J, et al. Whole-exome sequencing of polycythemia vera revealed novel driver genes and somatic mutation shared by T cells and granulocytes. *Leukemia.* 2014;28(4):935-938.
5. Ortmann CA, Kent DG, Nangalia J, et al. Effect of mutation order on myeloproliferative neoplasms. *N Engl J Med.* 2015;372(7):601-612.
6. Nussenzveig RH, Swierczek SI, Jelinek J, et al. Polycythemia vera is not initiated by JAK2V617F mutation. *Exp Hematol.* 2007;35(1):32.e1-32.e9.
7. Kralovics R, Teo SS, Li S, et al. Acquisition of the V617F mutation of JAK2 is a late genetic event in a subset of patients with myeloproliferative disorders. *Blood.* 2006;108(4):1377-1380.
8. Wang L, Swierczek SI, Lanikova L, et al. The relationship of JAK2(V617F) and acquired UPD at chromosome 9p in polycythemia vera. *Leukemia.* 2014;28(4):938-941.
9. Kumar P, Henikoff S, Ng PC. Predicting the effects of coding non-synonymous variants on protein function using the SIFT algorithm. *Nat Protoc.* 2009;4(7):1073-1081.
10. Tavtigian SV, Deffenbaugh AM, Yin L, et al. Comprehensive statistical study of 452 BRCA1 missense substitutions with classification of eight recurrent substitutions as neutral. *J Med Genet.* 2006;43(4):295-305.
11. Ramensky V, Bork P, Sunyaev S. Human non-synonymous SNPs: server and survey. *Nucleic Acids Res.* 2002;30(17):3894-3900.
12. Schwarz JM, Cooper DN, Schuelke M, Seelow D. MutationTaster2: mutation prediction for the deep-sequencing age. *Nat Methods.* 2014;11(4):361-362.
13. Wallweber HJ, Tam C, Franke Y, Starovasnik MA, Lupardus PJ. Structural basis of recognition of interferon-α receptor by tyrosine kinase 2. *Nat Struct Mol Biol.* 2014;21(5):443-448.
14. Ma L, Clayton JR, Walgren RA, et al. Discovery and characterization of LY2784544, a small-molecule tyrosine kinase inhibitor of JAK2V617F. *Blood Cancer J.* 2013;3:e109.
15. Levine RL, Wadleigh M, Cools J, et al. Activating mutation in the tyrosine kinase JAK2 in polycythemia vera, essential thrombocythemia, and myeloid metaplasia with myelofibrosis. *Cancer Cell.* 2005;7(4):387-397.
16. Etheridge SL, Cosgrove ME, Sangkhae V, et al. A novel activating, germline JAK2 mutation, JAK2R564Q, causes familial essential thrombocytosis. *Blood.* 2014;123(7):1059-1068.

17. Marty C, Saint-Martin C, Pecquet C, et al. Germ-line JAK2 mutations in the kinase domain are responsible for hereditary thrombocytosis and are resistant to JAK2 and HSP90 inhibitors. *Blood.* 2014;123(9):1372-1383.

18. Mead AJ, Rugless MJ, Jacobsen SE, Schuh A. Germline JAK2 mutation in a family with hereditary thrombocytosis. *N Engl J Med.* 2012;366(10):967-969.

19. Kapralova K, Horvathova M, Pecquet C, et al. Cooperation of germline JAK2 mutations E846D and R1063H in hereditary erythrocytosis with megakaryocytic atypia. *Blood.* 2016;128(10):1418-1423.

20. Zhao L, Ma Y, Seemann J, Huang LJ. A regulating role of the JAK2 FERM domain in hyperactivation of JAK2(V617F). *Biochem J.* 2010;426(1):91-98.

21. Funakoshi-Tago M, Pelletier S, Moritake H, Parganas E, Ihle JN. Jak2 FERM domain interaction with the erythropoietin receptor regulates Jak2 kinase activity. *Mol Cell Biol.* 2008;28(5):1792-1801.

22. Witzig TE, Price-Troska TL, Stenson MJ, Gupta M. Lack of JAK2 activating non-synonymous mutations in diffuse large B-cell tumors: JAK2 deregulation still unexplained. *Leuk Lymphoma.* 2013;54(2):397-399.

23. Hudson AM, Yates T, Li Y, et al. Discrepancies in cancer genomic sequencing highlight opportunities for driver mutation discovery. *Cancer Res.* 2014;74(22):6390-6396.

24. Olcaydu D, Harutyunyan A, Jäger R, et al. A common JAK2 haplotype confers susceptibility to myeloproliferative neoplasms. *Nat Genet.* 2009;41(4):450-454.

25. Pearse RN, Feinman R, Ravetch JV. Characterization of the promoter of the human gene encoding the high-affinity IgG receptor: transcriptional induction by gamma-interferon is mediated through common DNA response elements. *Proc Natl Acad Sci USA.* 1991;88(24):11305-11309.

DOI 10.1182/blood-2016-04-711283

To the editor:

Acute myeloid leukemia with *TP53* germ line mutations

Armin Zebisch,[1] Ridhima Lal,[1] Marian Müller,[1] Karin Lind,[1] Karl Kashofer,[2] Michael Girschikofsky,[3] David Fuchs,[4] Albert Wölfler,[1] Jochen B. Geigl,[5] and Heinz Sill[1]

[1]Division of Hematology and [2]Institute of Pathology, Medical University of Graz, Graz, Austria; [3]Department of Internal Medicine I, Hospital Elisabethinen, Linz, Austria; [4]Department of Internal Medicine 3–Hematology and Oncology, Kepler University Hospital, Linz, Austria; and [5]Institute of Human Genetics, Medical University of Graz, Graz, Austria

Acute myeloid leukemia (AML) is considered a sporadic disease caused by sequential accumulation of somatically acquired mutations in hematopoietic stem or progenitor cells (HSPCs). However, familial clustering of myeloid neoplasms is being increasingly observed and attributed to highly penetrant germ line variants in several different genes.[1] The recently published "2016 revision to the World Health Organization (WHO) classification of myeloid neoplasms and acute leukemia" incorporated these findings and defined "Myeloid neoplasms with germ line predisposition" as a distinct disease entity.[2] In addition to a series of developmental syndromes, this group currently comprises cases with germ line mutations in *CEBPA*, *DDX41*, *RUNX1*, *ANKRD26*, *ETV6*, and *GATA2*. Here, we describe familial clustering of AML in a *TP53* mutated Li-Fraumeni syndrome (LFS) pedigree. Further screening of 186 primary AML specimens revealed the presence *TP53* germ line mutations in 1.1% of cases. Finally, we report their frequent occurrence in therapy-related AML (tAML) arising after antecedent ionizing radiation, an observation of relevance for future studies within this area. The study was approved by the ethical committee of the Medical University of Graz, Graz, Austria (vote numbers 21-065 ex 09/10 and 26-369 ex 13/14, respectively) and performed in accordance with the Declaration of Helsinki.

A 46-year-old white woman presented with tAML with a complex karyotype arising after previous administration of chemo- and radiotherapy for papillary thyroid carcinoma at the age of 26, colorectal cancer at the age of 30, and bilateral breast cancer at the age of 31 and 41 years, respectively. Despite 3 lines of intensive AML induction/salvage therapy, the patient never achieved remission and died of progressive disease 7 months after diagnosis. Personal and family history indicated an LFS according to Chompret criteria[3] (Figure 1). Interestingly, in addition to the characteristic LFS tumor spectrum, secondary AML following myelodysplasia was observed in the index patient's father and chronic myeloid leukemia was observed in one of her brothers. Analysis of the *TP53* gene was performed using skin fibroblasts and peripheral blood, respectively, as previously described.[4,5] A *TP53*

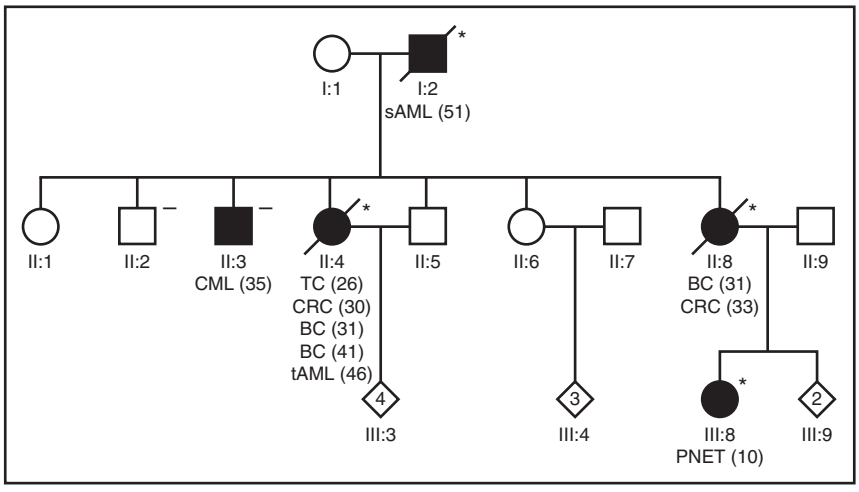

Figure 1. An LFS pedigree showing for the first time familial clustering of AML. The index patient developed tAML (II:4) following cytotoxic treatment of diverse antecedent malignancies, and the index patient's father (I:2) developed sAML following myelodysplasia. Filled symbols, subjects with malignancies; asterisk denotes a *TP53* c.467G>C, p.R156P germ line mutation carrier; the "minus" denotes a wild-type *TP53* germ line status. Numbers in brackets indicate age at diagnosis in years. BC, breast cancer; CML, chronic myeloid leukemia; CRC, colorectal cancer; PNET, primitive neuroectodermal tumor; TC, thyroid carcinoma.

2016 128: 2266-2270
doi:10.1182/blood-2016-04-711283 originally published online September 19, 2016

Coexistence of gain-of-function *JAK2* germ line mutations with *JAK2* ^{V617F} in polycythemia vera

Lucie Lanikova, Olga Babosova, Sabina Swierczek, Linghua Wang, David A. Wheeler, Vladimir Divoky, Vladimir Korinek and Josef T. Prchal

Blood (print ISSN 0006-4971, online ISSN 1528-0020), is published weekly by the American Society of Hematology, 2021 L St, NW, Suite 900, Washington DC 20036.

SUPPLEMENTARY METHODS

Patients

A total of 31 PV patients were collected for the research study. The collection of blood samples was performed at the University of Utah, School of Medicine, and was approved by the Institutional Review Board. Written consent was obtained from all patients in accordance with the Declaration of Helsinki. The LeukemiaNet criteria for clinical hematologic response were used to assess treatment response in patients.

DNA and RNA isolation

Granulocyte (GNC) and mononuclear cell fractions were isolated using Histopaque (Sigma-Aldrich, St. Louis, MO) density gradient centrifugation. T-cells were positively selected from mononuclear cells using the CD3+ MicroBead Kit (Miltenyi Biotec Inc, Auburn, CA). Genomic DNA was isolated from granulocytes and T-cells using the Gentra-Puregene Kit (Qiagen, Valencia, CA). DNA from nails was isolated using the QIAamp® DNA Mini Kit (Qiagen, Valencia, CA). RNA was isolated from the patient's granulocytes and BFU-Es using TRI reagent and residual DNA was removed by DNA-free DNase Treatment & Removal Reagents (Ambion, Life Technologies, NY).

Whole exome sequencing

Illumina library construction, exome capture, Illumina sequencing, exome sequencing data processing and quality control, mutation calling and annotation were previously described[1,2]. Mutation validation was done using the Ion Torrent Personal Genome Machine (PGM, Life Technologies Corporation). The Ion Torrent sequencing data were analyzed using Torrent Suite Software v3.0. DNA. The average read depth obtained per base was 2226x and 2034x for GNC and T-cells pools, respectively.

JAK2 molecular analysis

The *JAK2*^{V617F} mutational burden in granulocytes and BFU-Es was determined by quantitative allele-specific PCR (qAS-PCR).[3] The amplification of the exon 4 (T108A) and 9 (L393V) was done using the HotStarTaq Master Mix Kit (Qiagen, Valencia, CA) and the purified products were sequenced at University of Utah, Core DNA Sequencing Facility. Aliquots of DNA-free RNA were reverse-transcribed with SuperScript VILO (Invitrogen) and cDNA was amplified spanning the exon 4 – 16 and cloned into the pCR2.1-TOPO vector (TOPO TA Cloning kit; Invitrogen). Single colonies positive for the recombinant plasmid were picked after overnight incubation, plasmid DNA was purified using the QIAprep Spin Miniprep Kit (Qiagen, Valencia, CA) and the PCR insert was sequenced at University of Utah, Core DNA Sequencing Facility. *JAK2* 46/1 GGCC haplotype was determined on FastPCR 7500 instrument (Applied Biosystems) using Universal PCR Master Mix and TaqMan SNP assay on demand (rs3780367, C_27515396_10; rs10974944, C_31941696_10; rs12343867, C_319416 89_10), all samples were investigated in triplicate.

BFU-E analysis

Erythroid burst-forming unit colonies (BFU-E) were grown from peripheral blood mononuclear cells plated (2.3×10^5/mL) in methylcellulose media (MethoCult H4531; StemCell Technologies,

Vancouver, BC) without EPO. Cell cultures were maintained in humidified atmosphere of 5% CO2 at 37°C for 14 days. BFU-Es were scored by standard morphologic criteria. Individual BFU-Es were picked, genomic DNA and total RNA isolated, and their genotype was established as described above.

Characterization of cell lines

The Ba/F3-EPOR cell ($5x10^5$ cells per sample) were nucleofected with 2 μg pCMV6-AC-IRES-GFP-Puro "empty" vector or the construct encoding wt or mutated forms of JAK2 kinase using AMAXA II device (program X_001). Transfected cell were selected with 2 mg/mL puromycin for 2 weeks. The cells were grown in Dulbecco's modified Eagle medium supplemented with 10% fetal bovine serum (Invitrogen) and 1 U/mL EPO (StemCell Technologies). Proliferation of cells in the absence of EPO or in increased concentrations of EPO (0, 0.001, 0.01, 0.1 and 1 U/mL) was quantified by CellTitre-Blue reagent (Promega, Madison, WI) and Perkin-Elmer Envision analyzer. The dose-response curve for potent JAK2 inhibitor (LY2784544)[4] and IC50 was measured by CCK-8 proliferation assay (Sigma-Aldrich, St. Louis, MO) at 72 hours of exposure to different concentrations of LY2784544 in the presence of 1 U/mL EPO.

Dual luciferase transcriptional assays

STATs dependent transcriptional activity induced by JAK2 variants was measured using firefly luciferase STATs reporter (pGl4.26/GRR4.cz) in HCT116 cells. Reporter plasmid was constructed with STATs response elements[5], where single-stranded oligos (5'GAGATGTATTTCCCAGAAAA GGTTT) were annealed, ligated and cloned into the pGl4.26 reporter back-bone. The ratios of the constructs in the transfection mixtures (i.e. plasmids producing JAK2, EPOR, STATs, the luciferase reporter and the Renilla control vector, ratio: 2:1:0.3:0.3:0.3, respectively) were determined by titration experiments. The luciferase assay was performed according to the supplier's protocol using Dual-Glo Luciferase Assay System (Promega).

Western blot analysis

The level of human JAK2 protein in stably transfected Ba/F3-EPOR cell-lines was determined by western blot using anti-DDK antibody (Cell Signaling Technology, Danvers, MA). Ba/F3-EPOR cells expressing different JAK2 wt and mutant variants were cytokine-starved for 6 hours and then stimulated for 15 minutes. Western blots were performed with rabbit antibodies JAK2, pYJAK2 (Tyr 1007/1008), pYSTAT5 (Tyr 694), STAT5 (Cell Signaling Technology, Danvers, MA) and actin (Sigma-Aldrich, St. Louis, MO), which was used as a loading control. Signal was quantified using densitometric analysis.

References

1. Wang L, Swierczek S, Drummond J, et al. Whole-exome sequencing of polycythemia vera revealed novel driver genes and somatic mutation shared by T cells and granulocytes. *Leukemia*. 2014;28(4):935-938.
2. Wang L, Swierczek S, Lanikova L, et al. The relationship of JAK2(V617F) and acquired UPD at chromosome 9p in polycythemia vera. *Leukemia*. 2014;28(4):938-941.
3. Nussenzveig R, Swierczek S, Jelinek J, et al. Polycythemia vera is not initiated by JAK2V617F mutation. *Exp Hematol*. 2007;35(1):7.
4. Ma L, Clayton J, Walgren R, et al. Discovery and characterization of LY2784544, a small-molecule tyrosine kinase inhibitor of JAK2V617F. *Blood Cancer J*. 2013;3:e109.

5. Pearse R, Feinman R, Ravetch J. Characterization of the promoter of the human gene encoding the high-affinity IgG receptor: transcriptional induction by gamma-interferon is mediated through common DNA response elements. *Proc Natl Acad Sci U S A*. 1991;88(24):11305-11309.

Co-Occurring *JAK2* V617F and R1063H Mutations Increase JAK2 Signaling and Neutrophilia in MPN Patients

Cristina Mambet*[1,2,3], Olga Babosova*[4], Jean-Philippe Defour*[2,5], Emilie Leroy[1,2], Laura Necula[3], Oana Stanca[6,7], Aurelia Tatic[7,8], Nicoleta Berbec[6,7], Daniel Coriu[7,8], Monika Belickova[9], Barbora Kralova[10], Lucie Lanikova[4], Jitka Vesela[9], Christian Pecquet[1,2], Pascale Saussoy[5], Violaine Havelange[11], Carmen C. Diaconu[3], Vladimir Divoky[10,£] and Stefan N. Constantinescu[1,2,3,£]

1 Ludwig Institute for Cancer Research, Brussels Branch, Brussels, Belgium.
2 de Duve Institute, Université catholique de Louvain, Brussels, Belgium
3 MyeloAL Program, Stefan S Nicolau Institute of Virology, Bucharest, Romania
4 Department of Cell and Developmental Biology, Institute of Molecular Genetics, Academy of Sciences of the Czech Republic, Prague, Czech Republic.
5 Department of Clinical Biology, Cliniques universitaires Saint-Luc, Université catholique de Louvain, Brussels, Belgium.
6 Department of Hematology, Coltea Clinical Hospital, Bucharest, Romania.
7 Carol Davila University of Medicine and Pharmacy, Bucharest, Romania.
8 Center of Hematology and Bone Marrow Transplantation, Fundeni Clinical Institute, Bucharest, Romania.
9 Institute of Hematology and Blood Transfusion, Prague, Czech Republic
10 Department of Biology, Faculty of Medicine and Dentistry, Palacky University, Olomouc, Czech Republic
11 Service of Hematology, Cliniques universitaires Saint-Luc, Brussels, Belgium
*co-first authors
£ corresponding authors
Corresponding authors:
Stefan N. Constantinescu, Ludwig Institute for Cancer Research, Avenue Hippocrate 74, UCL 75-4, Brussels 1200, Belgium, stefan.constantinescu@bru.licr.org, Phone: +322-764-7540, Fax: +322-764-6566
and
Vladimir Divoky, Department of Biology, Faculty of Medicine and Dentistry, Palacky University, Hnevotinska 3, Olomouc, CZ-775 15, Czech Republic, vladimir.divoky@upol.cz Phone: +420-585632151; Fax: +420-585632966

While the concept of somatic driver mutations in myeloproliferative neoplasms (MPNs) represented by Polycythemia Vera (PV), Essential Thrombocythemia (ET) and Primary Myelofibrosis (PMF) is well established[1-3], the contribution of germline or co-occurring *JAK2* variants to a particular MPN phenotype is less understood.[4,5] Recently, two germline *JAK2* mutations, E846D and R1063H, were described in a case of hereditary erythrocytosis[6]; the same *JAK2* R1063H variant was initially reported in 3 out of 93 PV patients that were *JAK2* V617F-positive.[7]

In this study, we assessed the presence of *JAK2* V617F and *JAK2* R1063H mutations in a cohort of MPN patients, to characterize the double mutation carriers and gain insight into the functional consequences of coexisting mutations on JAK2 signaling.

Samples from 390 MPN patients positive for *JAK2* V617F from Romania (314) and Belgium (76) were collected for the study. *JAK2* R1063H mutation screening was performed using a custom TaqMan SNP Genotyping Assay. Fourteen out of 390 *JAK2* V617F-positive MPN patients were found to carry concurrently *JAK2* V617F and R1063H mutations. The clinical features and hematological data recorded at disease onset are summarized in Supplemental Table S1. ET was the most frequent diagnosis in double mutation carriers (9/14). After considering bone marrow histology and the new WHO 2016 criteria for PV diagnosis[8], 2 patients were reconsidered as having PV. Our major finding is that a significantly higher white blood cell count (P=0.023) and, correspondingly, a significantly higher neutrophil count (P=0.025) were observed in double mutation carriers compared to MPN patients harboring only *JAK2* V617F mutation (Figure 1A). When patients with ET diagnosis were analyzed separately, we found that carriers of both mutations displayed a significantly higher neutrophil count (P=0.031) and hemoglobin level (P=0.046) than V617F-positive ET patients (Supplemental Figure S1). Furthermore, in 5 patients there was at least one thrombotic event during the course of the disease, including 2 cases of portal vein thrombosis. Interestingly, in a recent genomic study of patients with venous thromboembolism, *JAK2* R1063H was identified in one case, being considered a probable disease-causing variant.[9]

To compare the frequency of additional somatic mutations in the analyzed patient groups, we employed a targeted next-generation sequencing (NGS) panel for the 14 double-mutated patients and for 53 randomly selected patients from the *JAK2* V617F cohort without the R1063H variant. Although a trend toward a higher mutational load was observed in the V617F/R1063H

group, compared to V617F group, the difference did not reach statistical significance (*P*=0.092) (Supplemental Table S2, Table S3).

Next, we aimed to characterize the genotype and configuration of *JAK2* mutations in the double-positive MPN patients. For these purposes, *JAK2* V617F and R1063H allelic burdens were analyzed by qPCR and digital droplet PCR (ddPCR) and *cis/trans* configurations of *JAK2* V617F and R1063H mutations were established by sequencing single colonies of sub-cloned JAK2 cDNA obtained from peripheral blood leukocytes in 10 out of 14 double-mutated patients. *Cis* configuration of the mutations was detected in 6 cases and *trans* configuration in 4 cases (Figure 1B). Quantification of R1063H allele in the genomic DNA samples indicated that the variant was heterozygous in 8 cases, likely inherited, as shown previously[6] (R1063H percentage about 50%). In 3 patients with high V617F allelic burden, R1063H was nearly homozygous (a fractional abundance >80%), suggesting that one R1063H allele was inherited and the second one was acquired by uniparental disomy (UPD). In 3 other patients who exhibited *trans* configuration of *JAK2* mutations (Figure 1B, supplemental Figure S2), low R1063H allele burden was found (allele percentage between 20.7% - 31.5%), raising the hypotheses that R1063H was either acquired in the course of the disease, or it was partially lost due to UPD of the V617F-non-R1063H clone which, when amplified, decreased R1063H allelic burden. Because non-myeloid tissue DNA was not available for the study, we used a combined array-comparative genomic hybridization/single-nucleotide polymorphism (aCGH/SNP) assay to detect unbalanced chromosomal changes and copy number neutral loss of heterozygosity in DNA samples with low R1063H allele burden. We detected UPD on chromosome 9p in 2 out of 3 samples, suggesting that both hypotheses could be valid (Supplemental Figure S3). However, without germline DNA, the origin of R1063H mutation cannot be unequivocally established.

Further on, cellular models were employed to assess the functional consequences of the coexisting *JAK2* mutations in *cis* or *trans*. We generated by site-directed mutagenesis JAK2 mutants (V617F, R1063H and V617F/R1063H) on the background of JAK2 cDNA cloned into pMEGIX-IRES-GFP bicistronic vector. STAT5 transcriptional activity of the JAK2 WT and JAK2 mutants in the presence of myeloid dimeric cytokine receptors (EPOR, TPOR, and G-CSFR) measured by dual luciferase assay led us to observe a significantly higher constitutive activity of JAK2 V617F/R1063H (*cis* mutant) compared to that of JAK2 V617F, in both homozygous and heterozygous configurations and with each cytokine receptor (Figure 2A-C).

Also, Western blot analysis demonstrated a higher level of constitutive activation of JAK2 and STAT5 induced by V617F/R1063H mutant versus V617F (Figure 2D). We then asked whether R1063H enhances the same conformational circuit used by V617F or triggers a different one. We introduced the E596R mutation in V617F/R1063H, as this mutation was previously found to block V617F-constitutive, but not ligand-induced JAK2 activity[10]. The constitutive STAT5 transcriptional activities of V617F and V617F/R1063H mutants were decreased to the same extent by E596R (Figure 2E). Thus, R1063H amplifies signaling via the same circuit as V617F.

The enhancement of G-CSFR signaling, which regulates neutrophilic granulocyte formation, by V617F/R1063H might be relevant for the neutrophilia, which is not seen in all MPN patients with JAK2 V617F. Neutrophilia is detected in the JAK2-double mutant patients, irrespective of *cis* or *trans* configuration. For the latter, we could not see an enhanced activation by R1063H and V617F versus WT JAK2 and V617F via cytokine receptors (Figure 2A-C), possibly as small changes are difficult to detect in overexpression systems. We assessed whether R1063H changes the association of JAK2 to G-CSFR. Using co-immunoprecipitation, we detected a significantly higher biochemical association between JAK2 R1063H and JAK2 V617F/R1063H with G-CSFR, when compared to JAK2 V617F or JAK2 (Figure 2F). This might have a significant impact on signaling at low receptor levels *in vivo*, and also in a *trans*-configuration, as R1063H alone enhances association of JAK2 with G-CSFR. Linking neutrophilia to the increased association of JAK2 V617F/R1063H to G-CSFR is in agreement with a recent study where differential coupling of JAK2 mutants to different receptors impacted the *in vivo* phenotypes induced by the different mutants.[12] In ET double-mutant carriers, the higher level of hemoglobin that accompanied the higher neutrophil count supports the hypothesis that co-occurrence of *JAK2* V617F and R1063H mutations would lead to an ET phenotype with PV-like features, due to a cumulative effect on JAK2 signaling.[15] Furthermore, the Ruxolitinib sensitivity of *JAK2* V617F/R1063H-expressing cells may have therapeutic implications (Figure 2G).

The frequency of R1063H in our *JAK2* V617F-positive MPN cohort (14/390) is consistent with the initial report (3/93 PV patients).[7] The frequency cited in the normal population for R1063H in the Exome Aggregation Consortium database[11] is much lower (0.004377). More studies on large patient populations, and on families with MPNs, would be necessary for determining whether *JAK2* R1063H predisposes to acquisition of the *JAK2* V617F

mutation, and also to assess its role in MPN progression, given the involvement of G-CSFR in leukemia.

ACKNOWLEDGEMENTS

We gratefully acknowledge the funding from the project Competitiveness Operational Program (COP) A1.1.4. ID: P_37_798, Contract 149/26.10.2016, (MySMIS2014+: 106774), MyeloAL Project. Funding to SNC is acknowledged from Ludwig Institute for Cancer Research, Fondation contre le cancer, Salus Sanguinis, Fondation Les Avions de Sébastien, ARC Project and WELBIO project, Belgium. OB, BK, LL and VD were supported by research funding from Czech Science Foundation, project GACR 17-05988S, and by Ministry of Education, Youth and Sports, Czech Republic (LO1220 project for OB and LTAUSA17142 project for BK, LL and VD). MB ad JV were supported by the project for conceptual development of research organization (00023736) MHCZ.

AUTHORSHIP CONTRIBUTIONS

CM, OB and JPD designed and performed research, analyzed data, and wrote the paper. LN, OS, AT, NB, DC, VH, PS and CCD recruited the patients, performed research and contributed to the editing of the paper. EL, BK, MB, JV, LL and CP performed research, analyzed data and reviewed the paper. SNC and VD designed the study, wrote the paper, and provided financial support.

DISCLOSURE OF CONFLICTS OF INTEREST

All authors declare no conflict of interest.

REFERENCES

1. Vainchenker W, Kralovics R. Genetic basis and molecular pathophysiology of classical myeloproliferative neoplasms. *Blood*. 2017;129(6): 667-679.

2. Skoda RC, Duek A, Grisouard J. Pathogenesis of myeloproliferative neoplasms. *Exp Hematol*. 2015;43(8):599–608.
3. Rumi E, Cazzola M. Diagnosis, risk stratification, and response evaluation in classical myeloproliferative neoplasms. *Blood*. 2017;129(6):680-692.
4. Harutyunyan AS, Kralovics R. Role of germline genetic factors in MPN pathogenesis. *Hematol Oncol Clin North Am*. 2012;26(5):1037-1051.
5. Lanikova L, Babosova O, Swierczek S, et al. Coexistence of gain-of-function JAK2 germ line mutations with JAK2 V617F in polycythemia vera. *Blood*. 2016;128(18):2266-2270.
6. Kapralova K, Horvathova M, Pecquet C, et al. Cooperation of germ line JAK2 mutations E846D and R1063H in hereditary erythrocytosis with megakaryocytic atypia. *Blood*. 2016;128(10):1418-1423.
7. Levine RL, Wadleigh M, Cools J, et al. Activating mutation in the tyrosine kinase JAK2 in polycythemia vera, essential thrombocythemia, and myeloid metaplasia with myelofibrosis. *Cancer Cell*. 2005;7(4):387-397.
8. Arber DA, Orazi A, Hasserjian R, et al. The 2016 revision to the World Health Organization classification of myeloid neoplasms and acute leukemia. *Blood*. 2016;127(20):2391-2405.
9. Lee EJ, Dykas DJ, Leavitt AD, et al. Whole-exome sequencing in evaluation of patients with venous thromboembolism. *Blood Advances*. 2017;1(16):1224-1237.
10. Leroy E, Dusa A, Colau D, et al. Uncoupling JAK2 V617F activation from cytokine-induced signalling by modulation of JH2 αC helix. *Biochem J*. 2016;473(11):1579-1591.
11. Lek M, Karczewski KJ, Minikel EV, et al. Analysis of protein-coding genetic variation in 60,706 humans. *Nature*. 2016;536(7616):285-291.
12. Yao H, Ma Y, Hong Z, et al. Activating JAK2 mutants reveal cytokine receptor coupling differences that impact outcomes in myeloproliferative neoplasm. *Leukemia*. 2017;31(10):2122-2131.
13. van den Akker EB, Pitts SJ, Deelen J, et al. Uncompromised 10-year survival of oldest old carrying somatic mutations in DNMT3A and TET2. *Blood*. 2017;127(11):1512-1515.
14. Hahn CN, Babic M, Schreiber AW, et al. Rare and common germline variants contribute to occurrence of myelodysplastic syndrome. *Blood*. 2015;126:1644 (ASH Meeting Abstract).

15. Campbell PJ, Scott LM, Buck G, et al. Definition of subtypes of essential thrombocythaemia and relation to polycythaemia vera based on JAK2 V617F mutation status: a prospective study. *Lancet (London, England)*. 2005;366(9501):1945–53.

A

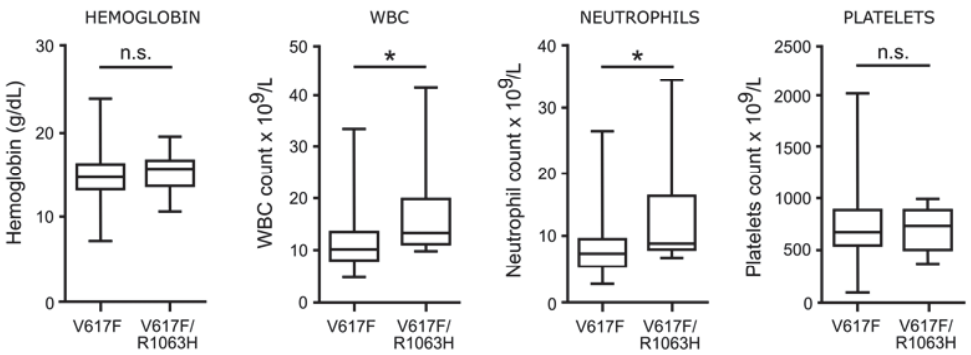

B

Patient	Diagnosis	*JAK2* V617F allele burden [%] (NGS/qPCR/ddPCR)	*JAK2* R1063H fractional abundance [%] (ddPCR)	*JAK2* VF/RH configuration	Additional mutations				
					Gene	Protein change	Type	Var Freq [%]	dbSNP ID
1	PV	66.6/56.4/64.2	9p UPD (20.7)	*trans*	***BCOR***	p.R411W	snv	54.0	NA
2	ET	9.6/8.8/11.1	heterozygous (50.8)	ND	***TET2***	p.G1187fs	insertion	3.1	NA§
3	ET	12.6/10.3/15.3	heterozygous (49.7)	ND	***not detected***				
4	ET	83.5/83.5/83.6	nearly homozygous (92.0)	*cis*	***DNMT3A***	p.Y365*	snv	3.7	NA§
					TET2	p.Y867H	snv	51.2	rs144386291#
5	PV	53.1/50.0/52.8	no 9p UPD (31.5)	*trans*	***not detected***				
6	ET	23.3/18.9/21.2	heterozygous (50.6)	ND	***not detected***				
7	ET	19.2/17.4/19.4	heterozygous (49.1)	*trans*	***not detected***				
8	PMF	26.8/23.7/25.4	heterozygous (50.5)	*cis*	***not detected***				
9	PMF	17.1/18.0/17.8	heterozygous (49.5)	*cis*	***TET2***	p.S1607*	snv	2.3	NA
10	PV	8.1/7.1/7.69	heterozygous (50.2)	*cis*	***DNMT3A***	p.D702Y	snv	9.1	NA20
					CBLB	p.V467I	snv	61.8	rs371993076#
					ZRSR2	p.R448_R449insSR	insertion	39.4	rs779595035#
11	ET	18.2/ND/16.4	heterozygous (49.7)	ND	***BCOR***	p.P1648L	snv	99.5	rs763651353
12	PV	73.2/72.7/73.2	nearly homozygous (84.5)	*cis*	***GATA2****	p.A164T	snv	57.5	rs2335052
13	PV	76.2/81.2/79.9	nearly homozygous (89.1)	*cis*	***not detected***				
14	ET	46.0/31.8/47.7	9p UPD (27.6)	*trans*	***EZH2***	p.C528S	snv	7.0	NA

Figure 1. Clinical characteristics, *JAK2* analysis and NGS screening for the MPN patients exhibiting *JAK2* V617F and *JAK2* R1063H mutations.

(A) Hematological data of *JAK2* V617F MPN patients (n = 390) subdivided according to the *JAK2* R1063H mutation status. Data for V617F only (n = 376) and V617F/R1063H double mutation carriers (n = 14) were recorded at diagnosis. For further information see also supplemental Material and Methods and Table S1. The boxes represent 25% to 75% interquartile range, horizontal lines within the boxes indicate medians, and vertical bars show the range of values (minimum to maxium). Mann-Whitney U test was used to assess the statistical significance. P values <0.05 were considered statistically significant.

(B) *JAK2* V617F allele burden, *JAK2* R1063H fractional abundance, *JAK2* V617F/R1063H mutations configuration and additional mutations identified by targeted NGS. (i) *JAK2* V617F allele frequency obtained from NGS study and compared with allele burden determined via qPCR and ddPCR assay. (ii) *JAK2* R1063H fractional abundance was determined using ddPCR in whole blood samples collected at the time of diagnosis (see supplemental Material and

Methods for details). The *JAK2* R1063H mutation was considered as genuine germline only when the fractional abundance of the *JAK2* R1063H variant was 50 (±1.0) %. Eight patients are therefore confirmed to be heterozygous germline carriers for *JAK2* R1063H variant. *JAK2* R1063H in three samples with percentage frequency of the mutant DNA between 20.7% - 31.5% (Samples no. 1, 5 and 14) could be considered as either acquired somatic mutation or an inherited variant that was partially lost due to UPD of the V617F-non-R1063H clone. Samples No. 4, 12 and 13 were nearly homozygous for *JAK2* R1063H and the presence of minor fraction of the wild-type allele excluded germline homozygosity. See also supplemental Figure S2. (iii) *cis*/*trans JAK2* V617F/R1063H mutations configuration was determined through sequencing of subcloned RT-PCR products spanning exons 14 – 24 of the *JAK2* gene (see supplemental Material and Methods for details). (iv) TruSight Myeloid Sequencing Panel (Illumina, San Diego, CA, USA) was used for targeted mutational screening of *JAK2* R1063H-positive patients. Additional mutations were identified in 8 out of 14 screened patients. A total of 11 variants in 7 genes were detected. Five of these mutations are indexed in the dbSNP database, and 4 of these specific variants are listed in the COSMIC catalogue (#). One additional mutation in *DNMT3A* was published recently.[13] Two other mutations (frameshift in *TET2* and premature stop codon in *DNMT3A*) do not have SNP/COSMIC IDs, but are documented on VarSome genomic variant database (§). The *GATA2* (A164T) allele (Patient 12) was recently detected in higher than expected frequency in MDS, suggesting a possible predisposing function in myeloid malignancies.[14] Two patients harbor unique undescribed variants, Patient 1 in *BCOR* and Patient 9 in *TET2*. The *BCOR* variants were identified in two patients (both are missense mutations); their variant frequency being of 54% for Patient 1 and 99.5% for Patient 11. They could be germ-line variants; both were estimated to be ‘damaging' or ‘probably damaging' by 2 algorithms (Sift, PolyPhen). All mutations were identified in DNA collected at the time of diagnosis; acquisition of additional mutations during disease evolution was not studied. For further information see supplemental Table S2. Abbreviations: PV, Polycythemia Vera; ET, Essential Thrombocythemia; PMF, Primary Myelofibrosis; NA, not available; ND, not done. DbSNP ID: ID in The Single Nucleotide Polymorphism database.

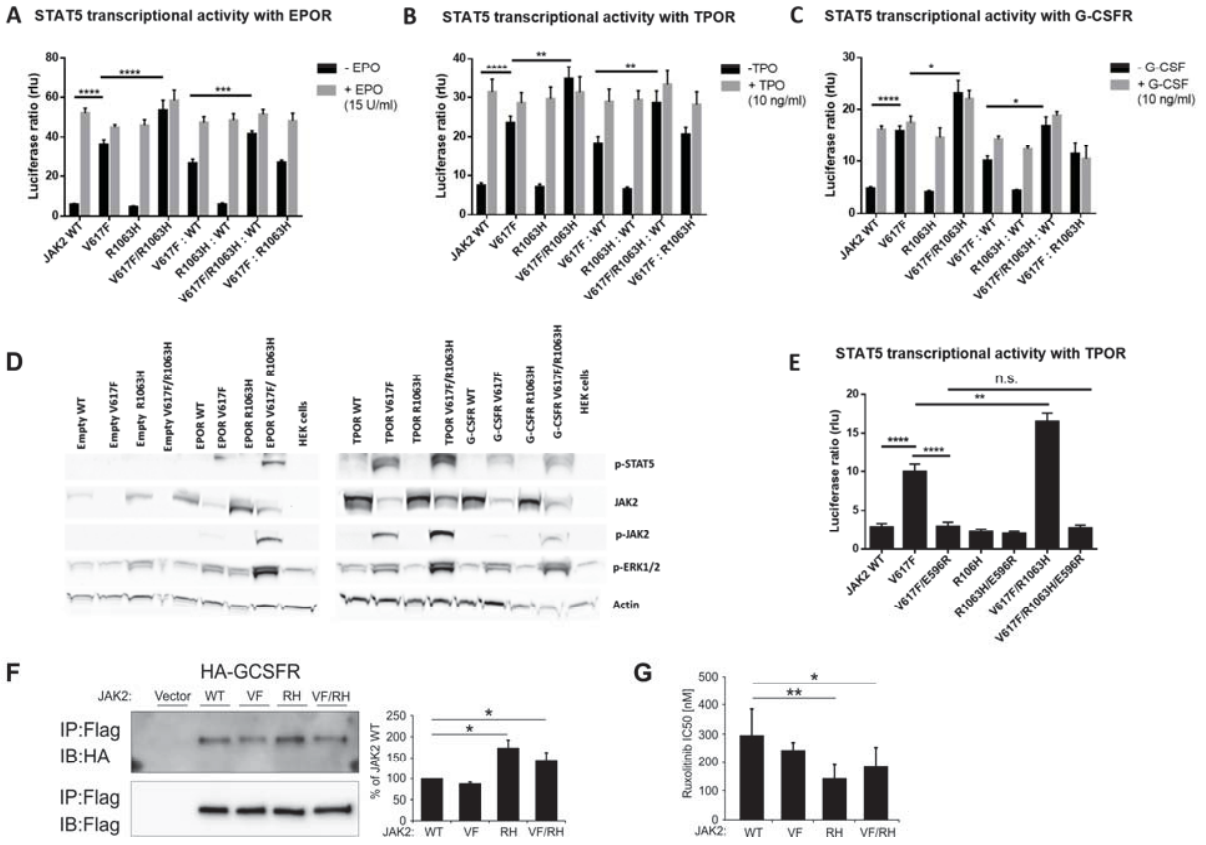

Figure 2. STAT5 transcriptional activity and the status of activation of downstream signaling by human JAK2 V617F and R1063H in the presence of dimeric myeloid cytokine receptors (A-E). The binding affinities of JAK2 mutants to G-CSFR (F) and *in vitro* drug sensitivity assay (G).

(A-C) Constitutive and cytokine-dependent STAT5 transcriptional activity assessed by dual-luciferase assay in γ2A cells transfected with JAK2 WT, JAK2 V617F, JAK2 R1063H, and JAK2 V617F/R1063H double mutant in the presence of EPOR (A), TPOR (B) and G-CSFR (C). Homozygous as well as heterozygous states of JAK2 mutants are mimicked. Shown are averages of nine replicates from three independent experiments ± standard error of the mean (SEM). Statistical analysis was assessed by one-way ANOVA followed by the post-hoc Tukey's test. *P <0.05, **P<0.01, ***P <0.001, ****P<0.0001. rlu: relative light unit.

(D) Western blot analysis of the constitutive JAK2, STAT5 and ERK 1/2 phosphorylation levels (indicative of activated status) induced by human JAK2 mutants co-expressed with empty vector/cytokine receptors in HEK 293T cells. β-actin antibody was used as a loading control.

Higher levels of p–JAK2 (p-Tyr1007/1008), p-STAT5 (p-Tyr694) and p-ERK ½ (p-Thr 202/p-Tyr 204) are observed in cells expressing JAK2 V617F/R1063H double mutant in comparison to JAK2 V617F. Image shown is representative of three independent experiments.

(E) The effect of E596R mutation on the constitutive STAT5 activation induced by JAK2 V617F and JAK2 V617F/R1063H evaluated by dual luciferase assay in γ2A cells in the presence of TPOR. Both mutated proteins exhibit a similar decline in constitutive activity. The graphs display the averages of nine replicates from three independent experiments ± standard error of the mean (SEM). One-way ANOVA followed by the post-hoc Tukey's test was used for statistical analysis. ****P<0.0001. n.s.: not significant, rlu: relative light unit.

(F) JAK2 mutants bind to cytokine receptor G-CSFR with different affinities. Flag-tagged JAK2 mutants were transiently expressed in HEK 293 cells in which HA-tagged G-CSFR was stably expressed. Interaction was examined by co-immunoprecipitation with anti-Flag affinity gel. Immunoblot band intensity was quantified by ImageJ software and normalized to a loading control, and wild-type JAK2 intensity was set to 100%. The data represent the mean of three independent experiments; T bars designate standard error of the mean (SEM). For statistical analysis Student's paired t test with equal variance was employed and P values <0.05 were considered statistically significant. WT: wild type, VF: V617F, RH: R1063H, VF/RH: V617F/R1063H, IP: immunoprecipitation. IB: immunoblot. See also supplemental Figure S4.

(G) *In vitro* drug sensitivity assay. Stably transfected Ba/F3/EPOR cells expressing JAK2 WT, JAK2 V617F, JAK2 R1063H, and JAK2 V617F/R1063H were cultivated for 72 hours with decreasing concentration of JAK2 inhibitor Ruxolitinib (concentrations: 1; 0.5; 0.25; 0.1; 0.05; 0.01; 0.001; 0 μM). The IC50 value was defined as drug concentration needed to inhibit 50% of cell growth (using GraphPad Prism 6.01 software). The data show mean of 7 independent experiments performed in triplicates (see also supplemental Material and Methods for details). T bars designate standard deviation (SD). When the Ruxolitinib sensitivity of mutant cells is compared to wild-type cells, the sensitivity of V617F-positive cells is not statistically significant, while R1063H-positive and V617F/R1063H double mutant cells are significantly more sensitive to Ruxolitinib than wild-type cells. Statistical significance was assessed using one-way ANOVA followed by post-hoc Tukey's test and P<0.05 was considered as statistically significant.

Experiments with AZ-960 revealed comparable results (not shown). WT: wild type, VF: V617F, RH: R1063H, VF/RH: V617F/R1063H.

Supplemental Materials and Methods, Tables, Figures and References for Mambet et al.

SUPPLEMENTAL MATERIAL AND METHODS

Patients and samples

Screening for the presence of *JAK2* R1063H was performed in 390 *JAK2* V617F-positive DNA samples, previously obtained by standard methods from peripheral blood granulocytes of MPN patients and stored in the biobanks of Stefan S Nicolau Institute of Virology, Bucharest, Romania, and Cliniques Universitaires Saint-Luc, Université catholique de Louvain, Belgium. The Romanian patients received an MPN diagnosis at the Hematology Services of Coltea and Fundeni Hospitals and were consequently referred to Stefan S Nicolau Institute of Virology for *JAK2* V617F mutation testing. All the patients included in the study provided informed consent at the time of blood drawing. Clinical data were analyzed retrospectively from the medical records of Coltea and Fundeni Hospitals and Cliniques Universitaires Saint-Luc, respectively.

Real-time PCR assay for *JAK2* R1063H mutation screening

To detect the *JAK2* R1063H mutation in the samples of genomic DNA (gDNA) we employed a custom TaqMan SNP Genotyping Assay (Applied Biosystems, Carlsbad, CA) with PCR primers flanking the mutant region and two allele-specific Taqman minor groove-binding (MGB) real-time PCR probes, performed on StepOnePlus Real-Time PCR System (Applied Biosystems).

Real-time quantitative PCR (qPCR) for *JAK2* V617F

The quantification of *JAK2* V617F mutation was performed using the ready-to-use ipsogen JAK2 MutaQuant Kit (Qiagen, Hilden, Germany) with a measured limit of detection of 0.1% on LightCycler® 480 Real-Time PCR instrument (Roche, Basel, Switzerland).

Next-generation sequencing for targeted mutational screening

In order to detect additional mutations of potential clinical relevance in MPN patients and to compare mutational load of patients harboring both *JAK2* V617F and R1063H mutations and *JAK2* V617F mutation only, we employed a targeted next-generation sequencing (NGS) panel (TruSight Myeloid Sequencing Panel, Illumina, San Diego, CA) for 14 *JAK2* V617F/R1063H double positive patients and for 53 randomly selected patients from the *JAK2* V617F cohort. The DNA libraries were generated from patients' granulocyte DNA according to the manufacturer instructions. The panel targeted 54 genes and covered full coding sequence of 15 genes and exonic hotspots of 39 genes. Targeted sequencing was performed on the Illumina MiSeq or NextSeq500 System using Illumina v3 Reagent Kit (600cycles) and V2 Mid OutPut Kit, respectively. We identified sequence alterations with a variant allele frequency (VAF) of ≥2%. The FASTQ files were analyzed by NextGENe V2.4.2.1 (SoftGenetics, State College, PA). The analysis included read quality trimming, alignment to the human hg19 reference genome, calling of single-nucleotide variants and short insertions or deletions. Read alignment and variant calling were also performed using the MiSeq Reporter (MSR) V2.6.3 software (Illumina), and annotated using VariantStudio V2.2 (Illumina). *JAK2* V617F allele frequency

was also obtained from NGS to allow comparison with digital droplet PCR (ddPCR) assay and qPCR.

Digital droplet PCR for *JAK2* R1063H and *JAK2* V617F allele burden measurement

To calculate the *JAK2* R1063H/wild type and *JAK2* V617F/wild type allele ratios, ddPCR was employed. One reaction of ddPCR was performed using 100 ng of genomic DNA, 1 µl of ddPCR™ Mutation Detection Assay mix for human *JAK2* R1063H/WT (20x assay mix, custom designed: dHsaMDS460320799; Biorad) or 1 µl of each probe PrimePCR™ ddPCR™ Mutation Assay for human *JAK2* V617F/WT (*JAK2* WT for p.V617: dHsaCP2000062 and *JAK2* p.F617: dHsaCP2000061; Biorad), 10 µl ddPCR™ Supermix for Probes (No dUTP; Biorad) and 1 µl of restriction enzyme *HindIII* (Thermo Scientific™) in total of 20 µl of reaction. Droplets were created using Droplet Generation Oil for Probes in QX200™Droplet Generator. PCR was performed in C1000 Touch™Thermal Cycler using conditions as follows, 95 °C for 10 min, 40 cycles of 30 s at 94 °C and 1 min at 55 °C, and a final step at 98 °C for 10 min. The ramp rate was always limited for 2 °C/sec. After the PCR reaction, droplet florescence was measured by QX200 Droplet Reader. Data were analyzed using QuantaSoft (Bio-Rad, V1.7.4).

***Cis/trans* configuration of *JAK2* V617F and R1063H mutations**

Patients' DNA-free RNA isolated either from whole blood or from peripheral blood leukocytes using Aurum™ Total RNA Mini Kit; Biorad and TRIzol method, respectively, was reverse transcribed by High Capacity cDNA Reverse Transcription Kit (Thermo Fisher Scientific). The position of V617F mutation relative to R1063H mutation was determined by amplifying a region spanning exons 14 – 24 of *JAK2* gene. The semi-nested PCR using primers (1st round, F1 5' ACGGTCAACTGCATGAAACA 3', R1 5' AGGAGGGGCG TTGATTTACA 3'; 2nd round, R2 5' ATCTCATCTGGGCATCCATC 3') was performed. The amplicon was gel-purified using Zymoclean™ Gel DNA Recovery Kit (Zymo Research) and cloned into pGEM-T easy vector (Promega). Single colonies positive for the recombinant plasmid were picked after overnight incubation, plasmid DNA was purified using the High Pure Plasmid Isolation Kit (Roche) and the PCR insert was sequenced at SEQme company, Czech Republic. At least 20 colonies per each amplicon (patient sample) were analyzed.

Microarray analysis for detection of chromosomal changes

Microarray analysis (array-comparative genomic hybridization/single-nucleotide polymorphism [aCGH/SNP]) was performed with SurePrint G3 Cancer CGH+SNP Microarray, 4x180K (Agilent Technologies, Santa Clara, CA) to detect unbalanced chromosomal changes and copy number neutral loss of heterozygosity (CN-LOH). The minimal resolution for the detection of CN-LOH was a region of ~3 Mb, which was achieved with approximately 20 SNP probes per Mb. The final product was scanned with the Agilent G2565CA Microarray Scanner System (Agilent) and analyzed with Agilent Cytogenomics v4.0.3.12 (Agilent).

Mutagenesis and vector construction

QuickChange II site-directed mutagenesis kit (Agilent Technologies, Santa Clara, CA) was used to introduce the *JAK2* c.1849G>T (V617F), and *JAK2* c.3188G>A (R1063H) point mutations into a human *JAK2* WT cDNA cloned in pMEGIX-IRES-GFP plasmid vector and also to generate double mutant *JAK2* c.1849G>T/*JAK2* c.3188G>A (V617F/R1063H), following the manufacturer instructions. Similarly, we introduced the suppressive E596R mutation for *JAK2* V617F into pMEGIX coding for human *JAK2* V617F, R1063H, and V617F/R1063H constructs. All JAK2 cDNA constructs were verified for accuracy by Sanger sequencing.

Dual luciferase assays for STAT5 transcriptional activity assessment

STAT5 transcriptional activity of the JAK2 WT and JAK2 mutants in the presence of myeloid dimeric cytokine receptors was measured in JAK2-deficient γ-2A fibrosarcoma cells[1] where we can reconstitute JAK2 or mutants, thereof. Dual luciferase assays were employed, using the firefly luciferase reporter Spi-Luc responding to STAT5 and p-RLTK renilla luciferase for normalizing transfection efficiencies, as previously described.[2] Briefly, γ-2A cells were transiently transfected with cDNA of JAK2 WT or mutants, Spi-Luc, STAT5, p-RLTK and either EPOR, TPOR or Granulocyte Colony-Stimulating Factor receptor (G-CSFR), at a 3:3:1:1:3 ratio, using Lipofectamine 2000 (Thermo Fisher Scientific, Waltham, MA). At the same time, to mimic heterozygous status encountered in patients, JAK2 V617F, R1063H, or V617F/R1063H mutants were co-transfected in γ-2A cells with an equal amount of JAK2 WT cDNA. Four hours after transfection, cell culture medium was changed and cells were incubated with the corresponding cytokine: 15 U/ml erythropoietin (EPO), 10 ng/ml thrombopoietin (TPO) or 10 ng/mL granulocyte colony-stimulating factor (G-CSF). 24 hours post-transfection the luciferase production was quantified in cell lysates with Dual-Luciferase® Reporter Assay kit (Promega, Madison, WI) on a Victor X luminescence microplate reader (Perkin Elmer, Waltham, MA). Firefly: Renilla luciferase ratios were calculated for each condition in order to assess the STAT5 transcriptional activity of different JAK2 constructs. In a similar manner, γ-2A cells were transfected with JAK2 E596R constructs and TPOR and dual-luciferase assay was applied to evaluate STAT5 constitutive activation.

Western blotting for signaling studies

Signaling studies were also performed in human embryonic kidney (HEK) 293T cells co-transfected with JAK2 WT or JAK2 mutants and one of the cytokine receptors, using TransIT®-LT1 Transfection Reagent (Mirus Bio, Madison, WI). After obtaining cell extracts, the levels of total JAK2 as well as the phosphorylation status of JAK2, STAT5, and extracellular signal-regulated kinase 1/2 (ERK1/2) were analyzed by western blotting with the following primary antibodies (all from Cell Signaling Technology, Danvers, MA): JAK2, phospho-Jak2 (p-Tyr1007/1008), phospho-Stat5 (p-Tyr694) and phospho-p44/42 MAPK (Erk1/2, p-Thr202/p-Tyr204).

Generation of cells stably expressing HA-tagged receptor

HA-tagged human G-CSFR cDNA was cloned in the retroviral pMX-IRES-GFP vector, as described previously.[4,5] The construct was co-transfected into retroviral producing cells HEK

293T together with the envelope encoding construct pCMV-VSV and Gag-Pol construct. Retroviral particles were collected at 48 and 72 hours after transfection and concentrated using filtration system Vivaspin® 20 (Sartorius). HEK 293 cells were then infected two times sequentially with the concentrated viral media overnight. Cells were GFP-sorted 72 hours after the second infection and the expression of G-CSFR was confirmed by Western blot.

Immunoprecipitation

HA-tagged receptor expressing HEK 293 cells cultured in DMEM + 10 % FBS and no additional cytokines, were transfected with pCMV-Puro-JAK2 variants using Lipofectamine 2000 (Thermo Fisher Scientific). 48 hours post transfection cells were lysed using lysis buffer (NaCl, Tris, Triton-X, CaCl2, MgCl2, EDTA) and a cocktail of proteinase inhibitors. For immunoprecipitation EZview™ Red ANTI-FLAG® M2 Affinity Gel (Sigma) was used according to the manufacturer's instructions. For maximal specificity elution using 3X FLAG® Peptide (Sigma) was performed. Receptors were detected using anti-HA rabbit monoclonal antibody (Cell Signalling, #3724) and JAK2 using anti-FLAG rabbit monoclonal antibody (Cell Signalling, #14793). Total cell lysates (TCL) were immunoblotted alongside the immunoprecipitated samples, anti-HA and anti-FLAG antibodies used for the detection are listed above, and a loading control anti-CtBP (Santa Cruz, sc-17759) was used.

***In vitro* Ruxolitinib sensitivity assay**

QuickChange II site-directed mutagenesis kit (Agilent Technologies, Santa Clara, CA, USA) was used to introduce *JAK2* c.1849G>T (V617F), *JAK2* c.3188G>A (R1063H) and combination of both *JAK2* c.1849G>T/*JAK2* c.3188G>A (V617F/R1063H) mutations into human *JAK2* WT ORF cDNA cloned in pCMV6-AC-IRES-GFP-Puro mammalian expression vector (OriGene, cat. no. PS100059). Ba/F3-EPOR cells cultured in IMDM medium containing 10% fetal bovine serum (FBS; both from Life Technologies) and 2 ng/mL of IL-3 (Sigma) were transfected with all the variants of pCMV-Puro-JAK2 vector by electroporation under conditions of 420 V and 250 μF using a Gene-Pulser (Bio-Rad, Hercules, CA). Stable transfectants were selected with 1 μg/ml puromycin (Life Technologies) for 2 weeks. *In vitro* drug sensitivity was determined using the MTT cytotoxicity assay, as described previously.[3]

Statistical analysis

Statistical tests were performed using GraphPad Prism 6.01 for Windows. Mann–Whitney U test was used to compare the differences in blood counts between the two groups of patients (double-mutation carriers and patients harboring only *JAK2* V617F mutation). One-way ANOVA followed by post-hoc Tukey's allowed for multiple comparisons between the measurements obtained by dual luciferase assays and *in vitro* Ruxolitinib sensitivity assay. Student's paired t test with equal variance was employed for assessing binding affinities of JAK2 mutants to G-CSFR. NGS data were compared and analyzed by the two-tailed Fisher exact test. Statistical significance was defined as $P < 0.05$.

SUPPLEMENTAL TABLES AND FIGURES

Table S1. Clinical data of *JAK2* V617F MPN patients (n = 390) subdivided according to the *JAK2* R1063H mutation status. Data for V617F only (n = 376) and V617F/R1063H double mutation carriers (n = 14) were recorded at diagnosis. Abbreviations: PV, Polycythemia Vera; ET, Essential Thrombocythemia; PMF, Primary Myelofibrosis; MPN-U, MPN Unclassifiable; WBC, White Blood Cell.

Variables	Patients JAK2 V617F/R1063H positive (n=14)	Patients JAK2 V617F positive (n=376)	*P* value
Sex ratio (male/female)	5/9	157/219	
Age, years, median (range)	60 (34-80)	61(16-92)	
MPN subtype (PV/ET/PMF/MPN-U)	5/7/2/0	115/205/34/22	
Hemoglobin g/dL, median (range)	15.8 (10.6 - 19.5)	14.7 (7.3 - 24.0)	0.43
WBC count × 10^9/L, median (range)	13.3 (9.9 - 41.6)	10.2 (4.6 - 31.6)	**0.023**
Neutrophil count × 10^9/L, median (range)	9.0 (6.9 - 34.2)	7.4 (2.6 – 26.8)	**0.025**
Platelet count × 10^9/L, median (range)	730 (363 - 1000)	670 (74 - 2025)	0.87
JAK2 V617F allele burden %, median (range)	21.3 (7.1 - 83.5)	32.0 (5.5 - 89.9)	0.78

Table S2. Detailed information about mutations identified by TruSight Myeloid Sequencing Panel for the MPN patients exhibiting *JAK2* V617F and *JAK2* R1063H mutations.

** Denotes likely inherited *GATA2* (A164T) variant, recently associated with increased risk of developing myeloid malignancy.[6]

Abbreviations: D, deleterious; PD, probably damaging; T, tolerated; B, benign; NA, not available. DbSNP ID: ID in The Single Nucleotide Polymorphism database. (1) This variant does not have SNP/COSMIC ID, but has been repeatedly viewed on VarSome.

SUPPLEMENTAL TABLE 2. for Mambet et al.

Patient	Diagnosis	Additional mutations										
		Gene	CDS mutation	Protein change	Chr	Type	Var Freq [%]	Var Type	Sift	PolyPhen	dbSNP ID	References
1	PV	***BCOR***	c.1231C>T	p.R411W	X	snv	54.0	missense	D	PD	NA	
2	ET	***TET2***	c.3556_3557insA	p.G1187fs	4	insertion	3.1	frameshift	NA	NA	NA	(1) www.varsome.com/variant
3	ET	***not detected***										
4	ET	***DNMT3A***	c.1095C>G	p.Y365*	2	snv	3.7	stop	NA	NA	NA	(1) www.varsome.com/variant
		TET2	c.2599T>C	p.Y867H	4	snv	51.2	missense	D	PD	rs144386291	COSM327337
5	PV	***not detected***										
6	ET	***not detected***										
7	ET	***not detected***										
8	PMF	***not detected***										
9	PMF	***TET2***	c.4820C>A	p.S1607*	4	snv	2.3	stop	NA	NA	NA	
10	PV	***DNMT3A***	c.2104G>T	p.D702Y	2	snv	9.1	missense	D	PD	NA	PMC4797027
		CBLB	c.1399G>A	p.V467I	3	snv	61.8	missense	T	B	rs371993076	COSM1035961
		ZRSR2	c.1314_1315insAGCCGG	p.R448_R449insSR	X	insertion	39.4	in-frame	NA	NA	rs779595035	COSM5762985
11	ET	***BCOR***	c.4943C>T	p.P1648L	X	snv	99.5	missense	D	PD	rs763651353	
12	PV	***GATA2****	c.490G>A	p.A164T	3	snv	57.5	missense			rs2335052	
13	PV	***not detected***										
14	ET	***EZH2***	c.1582T>A	p.C528S	7	snv	7.0	missense			NA	

Table S3. Detailed information about mutations identified by TruSight Myeloid Sequencing Panel for the *JAK2* V617F-positive/R1063H-negative patients in our cohort.

Additional mutations were identified in 12 out of 53 screened patients (after the exclusion of *GATA2* (A164T) SNP). A total of 17 variants in 8 genes were detected. Two of these mutations are indexed in the dbSNP database, and 7 of these specific variants are listed in the COSMIC catalogue (#). Seven patients harbor unique undescribed variants. ** Denotes likely inherited *GATA2* (A164T) variant (11 times in heterozygous and 2 times in homozygous configuration), recently associated with increased risk of developing myeloid malignancy.[6] In this cohort of 53 patients, the variant comprises 14% of allele frequency, which is consistent with the expected frequency (European non-Finnish 15% allelic frequency - http://gnomad.broadinstitute.org/variant/3-128204951-C-T; European 18% allelic frequency - https://www.ncbi.nlm.nih.gov/projects/SNP/snp_ref.cgi?rs=2335052). All mutations were identified in the genomic DNA collected at the time of diagnosis; acquisition of additional mutations during the disease evolution was not studied.

Abbreviations: PV, Polycythemia Vera; ET, Essential Thrombocythemia; PMF, Primary Myelofibrosis; NA, not available; dbSNP ID: ID in The Single Nucleotide Polymorphism database.

SUPPLEMENTAL TABLE 3. for Mambet et al.

Patient	Diagnosis	JAK2 V617F allele burden [%]	Gene	Protein change	Type	Var Freq [%]	dbSNP ID	
1	ET	4.0	not detected					
2	PMF	38.9	not detected					
3	PV	51.8	*GATA2***	p.A164T	snv	58.7	rs2335052#	COSM445531
4	ET	5.9	not detected					
5	PV	10.2	*ETV6*	p.R14*	snv	5.5	NA	
			*GATA2***	p.A164T	snv	56.7	rs2335052#	COSM445531
6	PMF	38.6	*GATA2***	p.A164T	snv	50.0	rs2335052#	COSM445531
7	PV	32.3	not detected					
8	PMF	19.5	*GATA2***	p.A164T	snv	99.1	rs2335052#	COSM445531
9	PV	83.1	not detected					
10	ET	10.6	*GATA2***	p.A164T	snv	48.9	rs2335052#	COSM445531
11	ET	5.4	*JAK2*	p.N542_E543del	deletion	10.0	NA#	COSM1757322
12	PV	54.7	not detected					
13	ET	34	not detected					
14	PV	46.6	*GATA2***	p.A164T	snv	56.3	rs2335052#	COSM445531
15	ET	18.6	*GATA2***	p.A164T	snv	47.5	rs2335052#	COSM445531
16	ET	8.4	not detected					
17	ET	14.9	not detected					
18	ET	38.9	not detected					
19	ET	19.8	*GATA2***	p.A164T	snv	49.0	rs2335052#	COSM445531
20	ET	18.1	not detected					
21	PMF	26.3	not detected					
22	ET	29.2	not detected					
23	PV	49.4	not detected					
24	PV	70.1	not detected					
25	ET	14.7	*GATA2***	p.A164T	snv	50.6	rs2335052#	COSM445531
26	PV	46.8	not detected					
27	PV	65.3	not detected					
28	ET	11.6	*ASXL1*	p.P805fs	deletion	6.8	NA	
29	ET	26.6	*KDM6A*	p.Q1377*	snv	4.6	NA#	COSM255009
30	PMF	41.2	*ZRSR2*	p.E362*	snv	89.1	NA#	COSM211059
			TET2	p.N377fs	deletion	10.4	NA	
31	PMF	91.6	not detected					
32	ET	18.6	not detected					
33	PMF	4.4	*KRAS*	p.R68S	snv	15.5	NA#	COSM183929
			SRSF2	p.H63P	snv	5.5	NA	
34	ET	12.3	not detected					
35	PV	22.1	not detected					
36	ET	13.5	*GATA2***	p.A164T	snv	56.8	rs2335052#	COSM445531
37	ET	28.0	not detected					
38	ET	32.8	*DNMT3A*	p.A884fs	deletion	35.3	NA	
39	PMF	19.9	*ASXL1*	p.P647fs	insertion	12.0	NA	
40	ET	13.8	not detected					
41	PMF	27.8	not detected					
42	PV	41.6	*TET2*	p.Q1030*	snv	45.8	rs780043982#	COSM4766113
43	ET	16.0	*GATA2***	p.A164T	snv	97.5	rs2335052#	COSM445531
44	early PV	23.3	*GATA2***	p.A164T	snv	48.4	rs2335052#	COSM445531
45	PV	80.3	*TET2*	p.D1384G	snv	18.2	NA#	COSM6023668
			DNMT3A	p.V897D	snv	17.8	NA#	COSM87000
46	PV	30.8	not detected					
47	ET	11.1	not detected					
48	ET	21.4	*GATA2***	p.A164T	snv	53.8	rs2335052#	COSM445531
49	PV	45.4	*TET2*	p.P1536fs	insertion	32.5	NA	
			TET2	p.L1065fs	deletion	12.8	NA	
			ASXL1	p.Q757*	snv	5.3	rs779078826#	COSM132979
50	PV	16.4	not detected					
51	ET	54.0	not detected					
52	PV	59.6	not detected					
53	ET	28.1	*TET2*	p.L1515*	snv	34.7	NA#	COSM5945064

Figure S1. Hematological data of *JAK2* V617F ET patients (n = 212) subdivided according to the *JAK2* R1063H mutation status. Data for V617F only (n = 205) and V617F/R1063H double mutation carriers (n = 7) were recorded at diagnosis. The boxes represent 25% to 75% interquartile range, horizontal lines inside the boxes indicate medians, and vertical bars show the range of values (minimum to maxium). Mann-Whitney U test was used to assess the statistical significance. P values <0.05 were considered statistically significant.

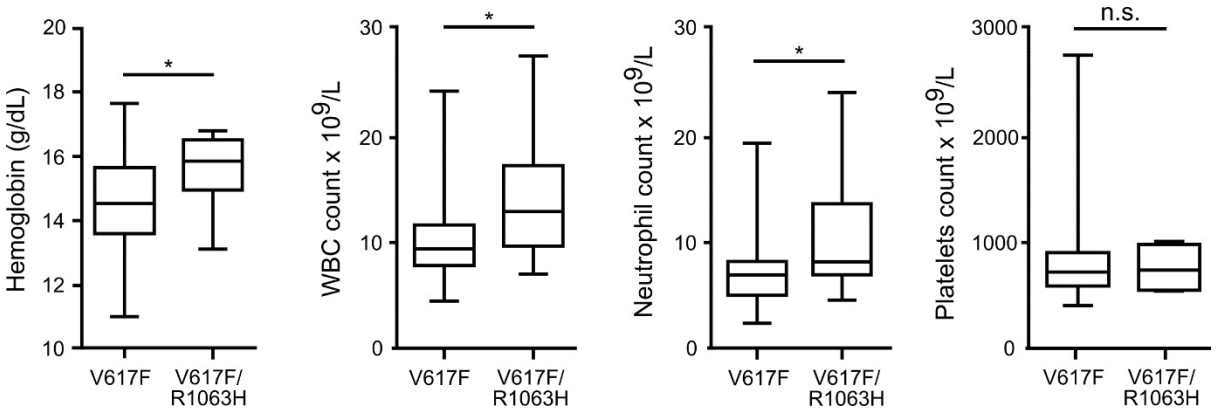

Figure S2. Quantification of *JAK2* R1063H allele in MPN patient samples using digital droplet PCR.

Single-well measurements of hybridization probes FAM/HEX specific for *JAK2* R1063H and *JAK2* WT were analyzed by QuantaSoft software and the count collection areas were held constant for each sampling.

(A) Comparison of number of events (amount of FAM- and HEX-positive droplets) of all analyzed patients. FAM fluorescence specific for the mutant allele is shown in blue while the HEX fluorescence specific for WT allele is shown in green.

(B) 2-D fluorescence amplitude plot generated by QuantaSoft software shows single-well measurement of a sample from one patient. The black cluster on the plot represents the negative droplets, the blue FAM cluster represents the droplets that are positive for the mutant DNA only, the green HEX cluster is specific for wild-type DNA only, and the orange cluster represents the droplets that are positive for both mutant and wild-type DNA. Patient 2 is presented as an example of a heterozygous sample compared to nearly homozygous sample obtained from Patient 4.

(C) Fractional abundance plot shows the percentage frequency of the mutant DNA in a wild-type DNA background. As presented in the boxplot, patients 1, 5 and 14 have low *JAK2* R1063H mutation allelic burden (20.7%, 31.5% and 27.6% of template copies detected carried

the mutation, respectively) and were examined for the presence of 9p UPD (see also Figure S3). Patients 4, 12 and 13 are nearly homozygous since 92.01%, 84.50% and 89.13% template copies carry the *JAK2* R1063H mutation, respectively. We hypothesize that one allele was inherited while the second one was acquired by UPD. This is also supported by the fact that allelic burden of *JAK2* V617F mutation in these patients is 83.5%, 73.2% and 76.2%, respectively. All the rest of the patients analyzed are heterozygous. All error bars generated by QuantaSoft software represent the 95% confidence interval.

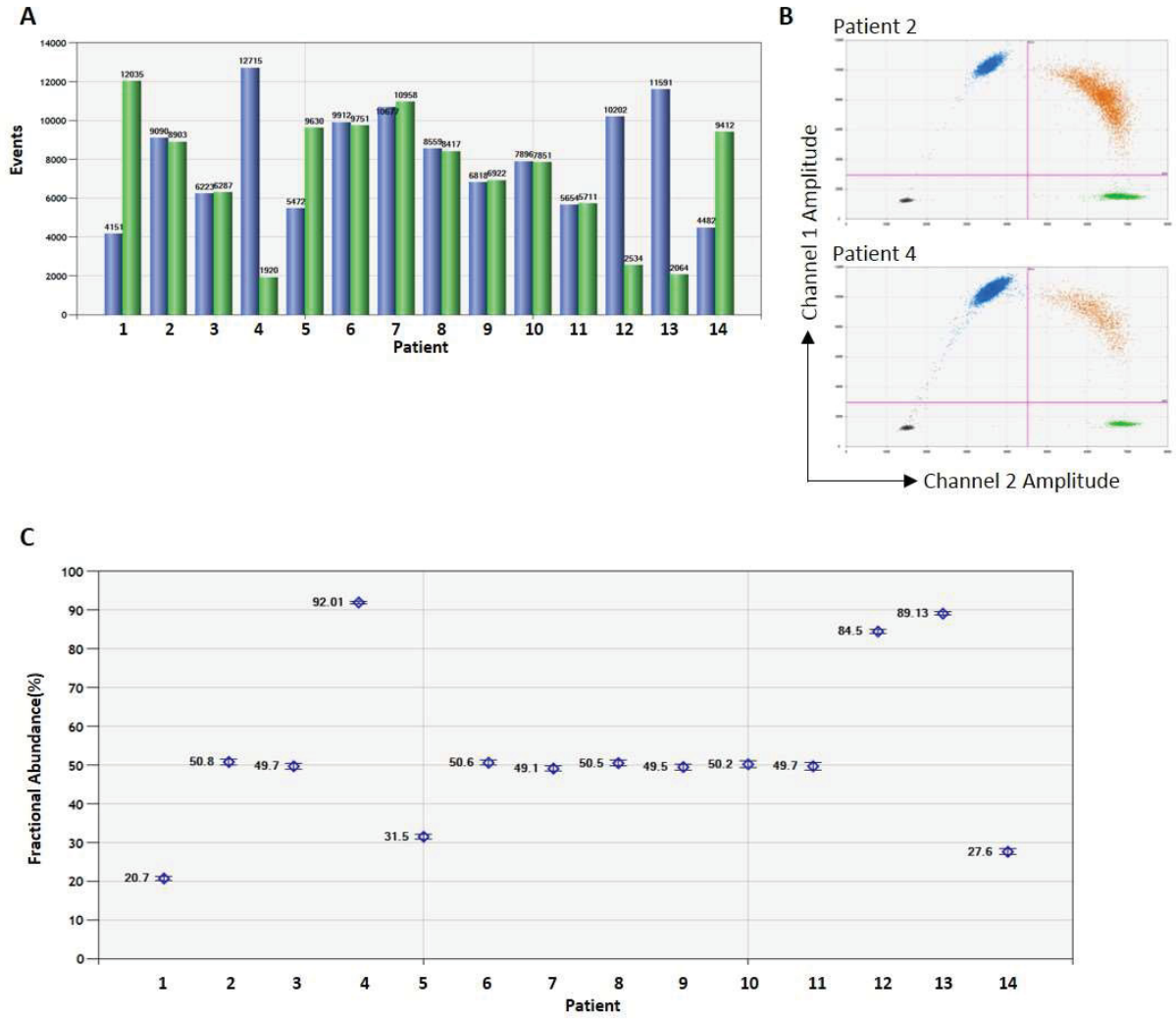

Figure S3. Determination of uniparental disomy for chromosome 9 of *JAK2* V617F positive MPN patients with low *JAK2* R1063H fractional abundance.

SNP-A based karyotypic analysis of chromosome 9 for patients with reduced fractional abundance of the *JAK2* R1063H was used to test hypothesis that the R1063H heterozygous germline variant carried by the non-V617F allele (in *trans* configuration) could have been lost due to mitotic recombination generating *JAK2* UPD of the V617F-non-R1063H clone which then could have been amplified thus leading to decreased R1063H allelic burden. Analysis was performed for patient #4 (nearly homozygous for both V617F and R1063H mutations, used as a positive control for UPD) and for patients #1, #5 and #14 with reduced fractional abundance

of the *JAK2* R1063H. Patient #4 (A) had cnLOH/UPD 9pterp21.3, patient #1 (B) carried cnLOH/UPD 9pterp21.2, patient #14 (C) carried cnLOH/UPD 9pterp21.1 at the detection limit and patient #5 (D) did not have detectable cnLOH/UPD 9p.

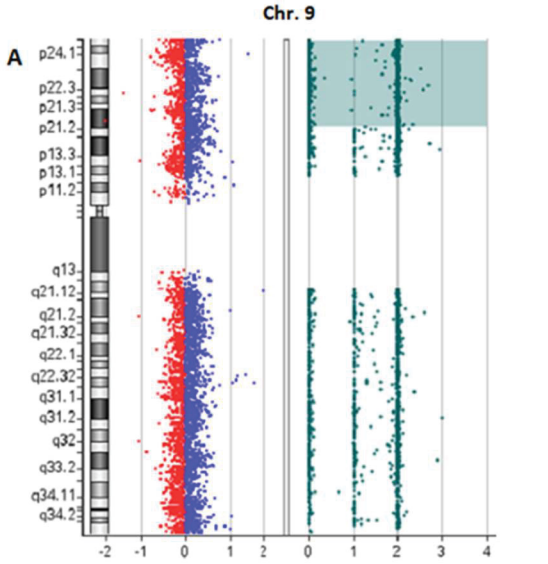

Patient #4: arr[GRCh37] 9pterp21.3 (404372_24957704)x2 hmz

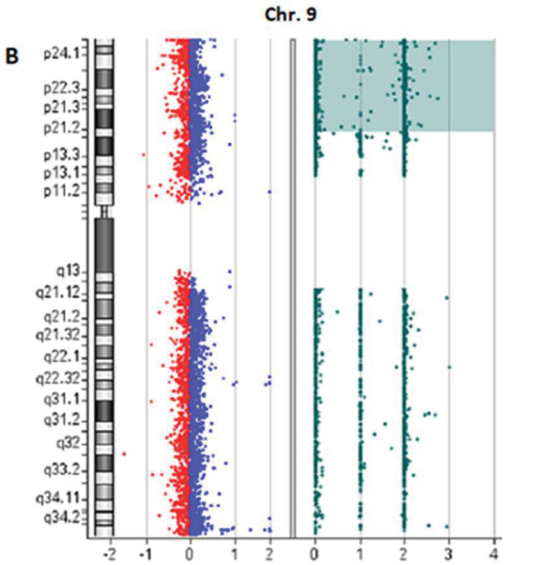

Patient #1: arr[GRCh37] 9pterp21.2 (558453_26530622)x2 hmz

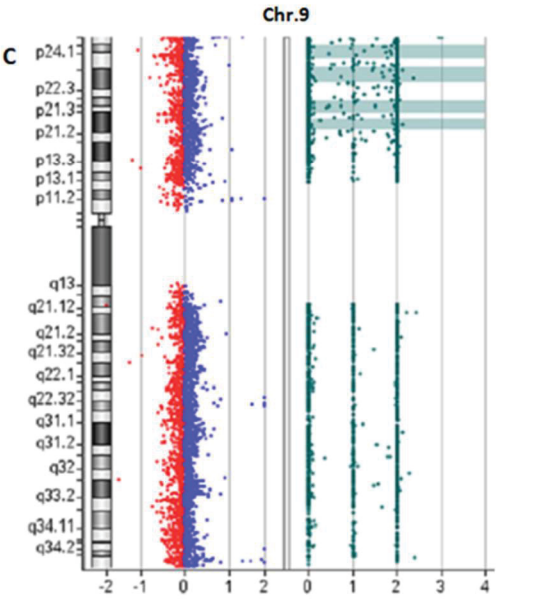

Patient #14: arr[GRCh37] 9p24.2p24.1(2389032_6134787)x2 hmz,
9p24.1p23(8250182_12316502)x2 hmz,
9p22.2p21.3(17147191_20076742)x2 hmz,
9p21.3(21720225_24566309)x2 hmz

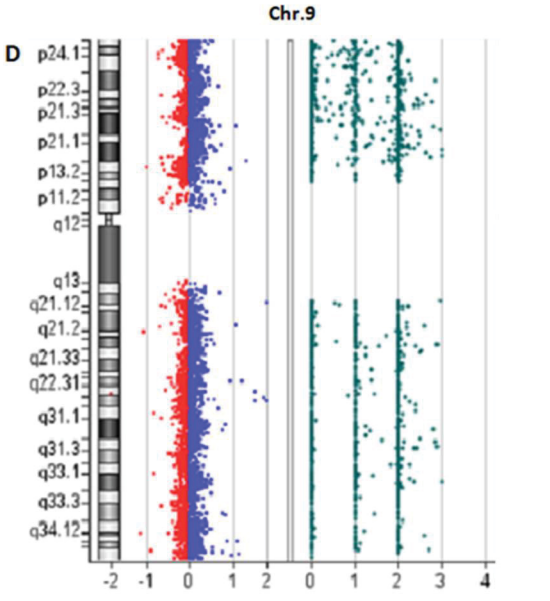

Patient #5: no UPD9p detected

Figure S4. Levels of HA-tagged G-CSFR and FLAG-tagged JAK2 in lysates are comparable when different JAK2 mutants are expressed in HEK 293 cells.

HEK 293 cells stably expressing HA-tagged G-CSFR were transfected with FLAG-tagged JAK2 variants and the total cell lysates (TCL) were extracted 24 hours post-transfection. TCL were immunoblotted alongside the immunoprecipitated samples. As a loading control CtBP protein was detected. WT: wild type, VF: V617F, RH: R1063H, VF/RH: V617F/R1063H.

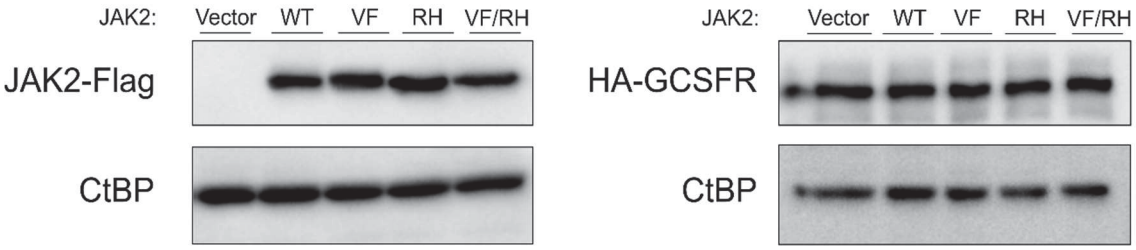

SUPPLEMENTAL REFERENCES

1. Kohlhuber F, Rogers NC, Watling D, et al. A JAK1/JAK2 chimera can sustain alpha and gamma interferon responses. *Mol. Cell. Biol* 1997; **17**: 695–706.
2. Defour J-P, Chachoua I, Pecquet C, Constantinescu SN. Oncogenic activation of MPL/thrombopoietin receptor by 17 mutations at W515: implications for myeloproliferative neoplasms. *Leukemia* 2016; **30**: 1214–1216.
3. Koledova Z, Kafkova LR, Calabkova L, et al. Cdk2 inhibition prolongs G1 phase progression in mouse embryonic stem cells. *Stem Cells Dev* 2010; **19**: 181-194.
4. Constantinescu SN, Liu X, Beyer W, et al. Activation of the erythropoietin receptor by the gp55-P viral envelope protein is determined by a single amino acid in its transmembrane domain. *EMBO J* 1999; **18**: 3334-3347.
5. Liu X, Constantinescu SN, Sun Y, et al. Generation of mammalian cells stably expressing multiple genes at predetermined levels. *Anal Biochem* 2000; **280**: 20-28.
6. Hahn CN, Babic M, Schreiber AW, Kutyna MM, Wee LA, Brown AL, et al. Rare and common germline variants contribute to occurrence of myelodysplastic syndrome. *Blood* 2015; **126**: 1644 (ASH Meeting Abstract).

The Role of Iron Chelation and 2-Oxoglutarate-Dependent Dioxygenase Inhibition in Regulation of Cyclin D1: Possible Therapeutic Implication for Mantle Cell Lymphoma

Olga Babosova[1], Katarina Kapralova[2,3], Vladimir Korinek[1], Vladimir Divoky[2], Josef T. Prchal[3], Lucie Lanikova[1,2,3]

[1] Department of Cell and Developmental Biology, Institute of Molecular Genetics, Academy of Sciences of the Czech Republic, Videnska 1083, 142 20 Prague 4, Czech Republic
[2] Department of Biology, Faculty of Medicine and Dentistry, Palacky University Olomouc, Hnevotinska 3, 775 00 Olomouc, Czech Republic
[3] Division of Hematology, University of Utah School of Medicine and VAH, Salt Lake City, UT 84132

Corresponding Authors:
Lucie Lanikova, PhD
Department of Cell and Developmental Biology
Institute of Molecular Genetics, Academy of Sciences of the Czech Republic
Videnska 1083,
142 20, Prague, Czech Republic
Phone: + 420241063107
Email: lucie.lanikova@img.cas.cz

and

Josef T. Prchal, MD
Division of Hematology
HCI RN 4126, 2000 Circle of Hope
University of Utah and HCI, Salt Lake City
UT 84112-5550 , USA
Phone: + 801-213-6013
Email: josef.prchal@hsc.utah.edu

Words Count: 3307
References: 44
Figures: 4

ABSTRACT (max. 240 words)

The majority of the patients with mantle cell lymphoma (MCL) have translocation t(11;14) leading to cyclin D1 overexpression and resulting in deregulated cell cycle control. We observed that iron depletion (an essential cofactor of prolyl hydroxylases (PHDs) blocked MCL cells' proliferation, induced cell cycle arrest and decreased cyclin D1 level. It was postulated that in cancer cells a loss of prolyl hydroxylase *EGLN2*/PHD1 leads to down-regulation of cyclin D1 by blocking the degradation of FOXO3A, a cyclin D1 suppressor. We tested whether inactivation of *EGLN2*/PHD1 in MCL cells would diminish cyclin D1 levels and whether inhibition of PHDs would impair MCL viability; this would have implications for MCL targeted therapy. We then asked whether cyclin D1 down-regulation in MCL by iron chelation is due to PHD1 inhibition and FOXO3A stabilization. Surprisingly, the CRISPR/Cas9 based loss-of-function of *EGLN2*/PHD1 in MCL cells did not affect cyclin D1 expression. In addition, loss of *FOXO3A* did not restore cyclin D1 levels after chelation treatment. These data suggest that expression of *cyclin D1* in MCL is not controlled by *ENGL2*/PHD1-FOXO3A pathway and that iron mediated down-regulation of cyclin D1 in MCL cells must be driven by another, yet unknown mechanism. Interestingly, MCL cell lines treated with prolyl hydroxylase inhibitor (DMOG) showed decreased proliferation and cyclin D1 level. Since DMOG is predicted to inhibit broad spectrum of dioxygenases it is likely that other 2-oxoglutarate-dependent enzymes have ability to regulate aberrantly expressed *cyclin D1* in MCL cells.

Keywords: mantle cell lymphoma, cell cycle, prolyl hydroxylases (*EGLN*/PHDs), 2-oxoglutarate-dependent enzymes, iron

INTRODUCTION

Mantle cell lymphoma (MCL) is an incurable B-cell lymphoma characterized by a translocation that juxtaposes the *CCND1* gene (which encodes *cyclin D1*, *CD1*) on chromosome 11q13 and an immunoglobulin heavy chain gene promoter on chromosome 14q32. MCL represents a small portion of malignant lymphomas, but it accounts for a disproportionately large percentage of lymphoma-related mortality. Despite a high rate of achieving complete remission (response rates 20-80%) by many chemotherapy regimens, the disease typically relapses after treatment with a median survival time of approximately 3-4 years.[1] Novel therapeutic approaches target several cellular pathways of MCL (CDK inhibitors, proteasome inhibitors, mTOR inhibitors, NFκB inhibitors and others), but so far have shown only modest effects on overall survival.[2] We observed that MCL-derived cell lines have decreased survival and proliferation compared to non-MCL when grown at iron deprived conditions[3] and Vazana-Barad et al.[4] reported that MCL patients may also benefit from iron chelator agents.

Iron is essential for cell proliferation[5], and although iron chelators were developed for treatment of iron overload diseases, they are also potent DNA synthesis inhibitors *in vitro*.[6] It has been shown that in MCL cell lines iron chelator deferasirox downregulates cyclin D1 which in turn leads to inhibition of Rb phosphorylation and increase of the E2F/Rb complex levels ultimately leading to G1/S arrest.[4] Other *in vitro* data demonstrate that iron chelation inhibits cell proliferation and induces apoptosis in breast cancer, renal carcinoma, neuroepithelioma and melanoma cell lines.[7] The mechanism by which iron may affect cancer cells has been suggested by Nurtjaha-Tjendraputra, et al[7] in a study that examined the ability of iron chelators to inhibit cell proliferation and induce apoptosis. It was postulated that iron chelation caused proteasomal degradation of cyclin D1. Interestingly, the degradation of cyclin D1 was ubiquitin independent in iron deplete conditions, while ubiquitination is important for cyclin D1 degradation in iron-repleted cells. The known ubiquitin independent protein degradation processes involve antizyme[8–10] and NAD(P)H-quinone oxidoreductase (NQO1).[10–12]

On the other hand, Zhang et al. showed that the mammalian cyclin D1-dependant proliferation is regulated by prolyl hydroxylase 1 (*EGLN2*/PHD1) in a hypoxia inducible factor (HIF)-independent manner by the transcriptional mechanism rather than via the proteasomal pathway.[13] Cyclin D1 is not a direct substrate for *EGLN2*/PHD1, but it was suggested that forkhead box O3A (FOXO3A) transcription factor is the link between the regulation of cyclin D1 and prolyl hydroxylase PHD1.[14] PHD1 can hydroxylate FOXO3A on two specific prolyl residues thereby blocking its interaction with the USP9x deubiquitinase and promoting its proteasomal degradation. Loss of *EGLN2*/PHD1 leads to accumulation of FOXO3A and consequently cyclin D1 is suppressed by FOXO3A.

The connection between prolyl hydroxylases and cell cycle regulation was first described in drosophila; their PHD homologue Hif-1 prolyl hydroxylase (Hph) was shown to be a regulator of cellular growth and a key mediator for the drosophila cyclin-dependent protein kinase complex cyclin D/cyclin-dependent kinase 4 (CycD/Cdk4).[15] Prolyl hydroxylases are the key oxygen sensors, there are three paralogues of the *EGLN* gene family (*EGLN1*/PHD2, *EGLN2*/PHD1 and *EGLN3*/PHD3), and are members of iron and 2-oxoglutarate-dependent dioxygenases family. In the cell, PHD1 was found to be exclusively present in the nucleus, PHD2 is mainly located in the

cytoplasm while PHD3 protein is homogenously distributed throughout the cytoplasm and nucleus.[16,17] All members of the PHD protein family contribute to regulation of cellular O_2 sensing, but only *EGLN2*/PHD1 and *EGLN3*/PHD3 were demonstrated to have HIF-independent functions, such as in DNA-damage control[18,19] and NF-κB activity.[20,21] The mouse PHD1 homologue *Falkor* was identified as a DNA damage related growth regulator in mouse embryonic fibroblasts.[21] It was shown that Falkor can also inhibit HIF-2α and that a combined knockout of PHD1 and PHD3, leads to erythrocytosis.[22,23] In human breast cancer cells, *EGLN2* mRNA was shown to accumulate in cells stimulated with estrogen and participate in estrogen-independent growth and resistance to hormone therapy.[24]

In the present study we confirmed the effect of cellular iron depletion on MCL cell lines[4,7] and observed increased sensitivity to chelation treatment of MCL cell lines in comparison to non-MCL cell lines which do not have constitutively active cyclin D1. Since the molecular mechanism inducing cyclin D1 degradation after iron chelation is not known, we assumed that it could be linked with *EGLN2*/PHD1-FOXO3A pathway. To further unravel role of prolyl hydroxylases in cyclin D1 regulation in MCL, we created MCL cell lines harboring the *EGLN2* or *FOXO3A* loss-of-function (LOF) genes. In addition, the MCL cells were treated with 2-oxoglutarate analog, dimethyl-oxalylglycine (DMOG), competitive inhibitor of prolyl hydroxylase domain-containing proteins, which has been used already in clinic and could open new avenue for MCL targeted therapy.

MATERIALS AND METHODS

Cell culture. Human MCL cell lines Jeko-1 and Mino were a kind gift from Dr. Jianguo Tao at the H. Lee Moffitt Cancer Center & Research Institute (Tampa, FL). The HBL-2 cell line were a kind gift from Dr. Elliot Epner at Oregon Health and Science University. We purchased SUDHL-6 (CRL-2959™), DG-75 (CRL-2625™) and HEK293 (CRL-1573™) from ATCC (Manassas, VA). All cell lines were maintained in RPMI medium 1640 with GlutaMAX (ThermoFisher Scientific), supplemented with 10% fetal bovine serum (ThermoFisher Scientific), and treated with 100 U/mL penicillin and 100 µg/mL streptomycin (both ThermoFisher Scientific) in a humidified atmosphere containing 5% CO_2 at 37°C. The treatments of the cells by deferoxamine mesylate salt (250 µM, DFO, Sigma Aldrich) and dimethyloxalylglycine (1 mM, DMOG, Sigma Aldrich) are indicated in the corresponding figures and legends. For hypoxia induction, cells were cultured 24 hours in hypoxia chamber (StemCell Technologies) containing certified gases mixture (1% O_2, 5% CO_2, 94% N_2), which was placed in the standard tissue culture incubator at 37°C.

Proliferation assay. Cell number and viability were determined using CellometerAutoT4 (Nexcelom Bio-science) based on the trypan blue exclusion method or by CellTitre-Blue reagent (Promega) and Perkin-Elmer Envision analyzer.

Cell cycle and apoptosis analysis. Cell cultures were synchronized by serum starvation as described elsewhere.[7] Briefly, cells were washed with PBS and serum-starved for 24 hours at 37°C. Starved cells were stimulated with 10% FBS for 16 hours at 37°C in the presence or absence of 250 µM DFO. Cells were harvested and washed with ice-cold PBS and fixed with 70% ethanol and the cell cycle was analyzed using a BD FACSCanto II flow cytometer (BD Biosciences) and FlowJo™ software. Apoptosis was evaluated by flow cytometry using an Annexin V-FITC Kit apoptosis detection kit (Miltenyi Biotec). Data were acquired by at least 10 000 cells using BD FACSCanto II instrument.

Western blot analysis. Cells were harvested to an ice cold RIPA buffer (Sigma-Aldrich) supplemented with a cocktail of protease inhibitors. Proteins were resolved on SDS-polyacrylamide gels and electro-blotted onto PVDF membranes (Millipore) or nitrocellulose membranes (Biorad). Membranes were incubated with following rabbit anti-human primary antibodies: cyclin D1 (#2922S, Cell Signaling, 1:1000), actin (Sigma-Aldrich, 1:1000), HSP90 (#4877, Cell Signaling, 1:2000), FOXO3A (#2497, Cell Signaling, 1:1000) and PHD1 (NB100-310, Novus Biologicals, 1:500); and mouse anti-human primary antibody CtBP (sc-17759, Santa Cruz, 1:1000) at 4°C overnight, washed in PBS with 0.05% Tween 20, and incubated for 1 hour with goat anti-rabbit or goat anti-mouse horseradish peroxidase (HRP)-conjugated secondary antibody (ThermoFisher Scientific). HRP activity was detected with an ECL detection kit (Pierce, ThermoFisher Scientific).

RNA isolation and quantitative RT-PCR. RNA was isolated using TRI reagent (Sigma Aldrich) and 500 ng of DNA-free RNA was reverse-transcribed using the First Strand cDNA Transcriptor Synthesis Kit (Roche) or 1000 ng of DNA-free RNA was reverse-transcribed using the RevertAid Reverse Transcriptase (Thermo Fisher Scientific) according to the manufacturer's manual. Gene expression experiments were performed on LightCycler 480 system (Roche) with following TaqMan probes: Hs00765553_m1 *CCND1,* Hs00153380_m1 *CCND2,* Hs00236949_m1 *CCND3*,

Hs00254392_m1 *EGLN1,* Hs00363196_m1 *EGLN2,* Hs00222966_m *EGLN3,* Hs00900055_m1 *VEGFA,* Hs00892681_m1 *SLC2A1,* Hs00175976_m1 *HK1,* Hs00818121_m1 *FOXO3A* and reference genes 4333761F *RPLP0* and 4333767F *GUSB*. All experiments were investigated in triplicate. The data reported represent the mean of three independent experiments; T bars designate SD. For statistical analysis Student's paired t-test with unequal variance was employed and P values <0.05 were considered statistically significant.

Plasmids, virus production and infection. Lentiviral LentiCas9-Blast (Addgene plasmid #52962) and LentiGuide-Puro (Addgene plasmid #52963) single guide RNA plasmids were processed according to Lentiviral CRISPR ToolBox protocol GeCKO. Briefly, 293T packaging cell line was used for LentiCas9 amplification using packaging plasmids pVSVg (Addgene #8454) and psPAX2 (Addgene #12260). The viruses were collected 24 hours after transfection, precipitated with PEG-it reagent (System Biosciences) and Mino cells were infected in the presence of 4 μg/ml Polybrene (hexadimethrine bromide) prior to drug selection (blasticidin 18 μg/ml) to produce cell line stably expressing Cas9 (Mino LentiCas9). The LentiCRISPR single guide RNA plasmid was digested by *BsmBI* enzyme, purified from agarose gel (Roche, High Pure PCR Product Purification Kit) and ligated with phosphorylated and annealed oligo pairs for single guide RNA (target sequence for *FOXO3A* 5' GTGGGTACGCACCTTCCAGC 3', for *EGLN2/PHD1* 5' *TGATGCAGCGCCCATCGCCG* 3'*).* Mino LentiCas9 cell line was infected as described above in the presence of 4 μg/ml Polybrene prior to drug selection (puromycin 1μg/ml).

RESULTS

The effect of cellular Fe depletion on human mantle cell and non-mantle cell lymphoma cell lines

In order to confirm that iron chelation inhibits cell growth and promotes apoptosis in MCL derived cell lines, human MCL cell lines Jeko-1, Mino and HBL-2 were treated with deferoxamine mesylate salt (DFO) using previously reported concentrations.[7] A 24- and 48-hour incubation with DFO decreased MCL viability (**Figure 1A, upper panel**) and increased apoptosis (**Figure 1A, lower panel**) of MCL cells. A possible cytotoxic effect due to a high concentration of DFO was ruled out by abrogating the effect by concomitant administration of ferric ammonium citrate (FAC) as co-incubation of cells with DFO and FAC had reverted the cytotoxic effect of DFO. Post-incubation with FAC after the pre-incubation with DFO also reversed the effect of iron chelation further demonstrating that the deprivation of iron is a cause of growth reduction and this iron effect is reversible (FAC added at 24 hours, data not shown). Treatment with FAC alone had no effect on cell growth or apoptosis (data not shown).

We then examined the iron depletion effect on the cell lines which do not have constitutively active cyclin D1, SUDHL-6 originating from diffuse large B-cell lymphoma and DG-75 isolated from Burkitt's lymphoma. Their growth after DFO treatment was decreased but not fully inhibited (growth rate of MCL vs. non-MCL cell lines at 48 hour time point is significantly different, $P < 0.05$) (**Figure 1B, left panels)** suggesting that the overexpression of cyclin D1 sensitizes MCL cell lines to treatment with DFO. The level of apoptosis after DFO treatment was comparable between non-MCL and MCL cell lines (**Figure 1B, right panel**).

All MCL cell lines had detectable levels of cyclin D1 at baseline; while under the same experimental conditions the expression of cyclin D1 in non-MCL cell lines was not detected. In MCL cell lines, cyclin D1 protein was no longer detectable on Western blot after 24 hours of incubation with DFO and FAC post-incubation fully restored the cyclin D1 protein level (**Figure 1C, left panel**).

In order to determine the iron chelation effect on the cell cycle progression, we synchronized MCL and non-MCL cells by serum starvation for 24 hours and then released the cells into the medium with 10% FBS or 10% FBS with DFO (protein levels of cyclin D1 are shown on **Figure 1C, right panel**). Cell cycle analysis revealed that MCL cell lines do not abrogate the cell cycle in the G1 phase under serum-starved conditions, suggesting that overexpression of cyclin D1 promotes cell proliferation (**Figure 1D**). In addition, the overexpression of cyclin D1 makes MCL cell lines more susceptible to treatment with DFO (percentage of G1 cells of MCL cell lines is significantly higher than in non-MCL cell lines, **Figure 1D**).

Despite the report[7] suggesting that *cyclin D1* mRNA is stable after iron chelation and its expression is regulated via the proteasome, DFO treatment of MCL cell lines decreased mRNA level of *cyclin D1* (**Figure 1E, left panel**). We also investigated the possible compensatory effect described by Klier et al[25], where a specific shRNA-mediated knockdown of *cyclin D1* mRNA had minimal effect on cell survival because of up-regulation of *cyclin D2* mRNA and protein expression. After treatment with DFO, we did not detect altered levels of either *cyclin D2* or *cyclin D3* mRNA (**Figure 1E, middle panel**). We further tested whether the DFO effect may be due to inhibition of one of the iron-dependent hypoxia-inducible factor hydroxylases. Expression analysis of MCL cell lines treated with DFO revealed down-regulation of PHD1 encoded by the *EGLN2* gene and up-regulation of *EGLN1*/PHD2 (**Figure 1E, right panels**).

Regulation of cyclin D1 in MCL cell lines is not controlled by *EGLN2*/PHD1 and its hydroxylation target FOXO3A

It has been previously reported that an inability of *EGLN2*/PHD1 to hydroxylate FOXO3A promotes its accumulation in cells, which in turn suppresses cyclin D1 expression by a yet unknown mechanism.[14] In order to decipher whether iron chelation downregulates cyclin D1 by inhibiting *EGLN2*/PHD1 function and thus prevents FOXO3A proteasomal degradation, we created *EGLN2*/PHD1 and FOXO3A CRISPR/Cas9 based loss-of-function MCL Mino cell lines (**Figure 2A, 2B**). The loss of *EGLN2*/PHD1 did not lead to the down-regulation of *cyclin D1* expression in MCL cell line (**Figure 2A, upper panels**). In order to validate our CRISPR/Cas9 system we created *EGLN2*/PHD1 LOF in HEK 293 cells and as expected, we observed down-regulation of *cyclin D1* on mRNA level (data not shown) suggesting that transcriptional regulation of *cyclin D1* in MCL cell lines is not controlled by *EGLN2*/PHD1.

We further examined the effect of iron chelation on cyclin D1 regulation in *EGLN2*/PHD1 and FOXO3A LOF cell lines. As expected, level of cyclin D1 was reduced on protein and also mRNA level after DFO treatment and restored when Fe source FAC was present in medium, in both edited cell lines (**Figure 2A, B**). As seen in **Figure 2B,** *FOXO3A* LOF in MCL line Mino did not prevent cyclin D1 down-regulation after DFO treatment (**protein level, 2B upper right panel; mRNA level, 2B lower panel)**. These data suggest that *FOXO3A* is not required for cyclin D1 repression in these cells and that cyclin D1 down-regulation in MCL cells after DFO treatment is not directly mediated by *EGLN2*/PHD1 hydroxylase. Interestingly, DFO treatment leads to up-regulation of *FOXO3A* transcript in parental Mino, CRISPR/Cas9 unedited cells. Up-regulation of *FOXO3A* was detected also in other MCL cell lines after DFO treatment (**Figure 2C**).

Down-regulation of *EGLN2* and accumulation of *FOXO3A* mRNA after DFO treatment in MCL cell lines is caused by induced hypoxia

Since DFO is a known hypoxia-mimetic agent we asked whether the down-regulation of cyclin D1 after DFO treatment is caused by induced hypoxia. First, we checked the expression of selected known HIF target genes (*VEGFA* and *SLC2A*); both were upregulated after DFO treatment in MCL cell lines (**Figure 3, upper left panel).** We then cultured MCL cell lines for 24 hours in hypoxia chamber with 1% O_2 atmosphere and performed expression analysis. While hypoxia effect was confirmed by expression of HIF target genes *VEGFA* and *SLC2A (***Figure 3, upper right panel***)* the level of *cyclin D1* was not significantly altered (**Figure 3, lower left panel**). However, the detected down-regulation of *EGLN2* and accumulation of *FOXO3A* mRNA (**Figure 3, lower panels**). It has been previously shown that *EGLN2* promoter contains binding sites for aryl hydrocarbon nuclear translocator (*ARNT*/HIF-1β)[26] which mediates its down-regulation under hypoxic conditions and that *FOXO3A* transcript level, in response to hypoxia, accumulates in HIF1-dependent manner, resulting in enhanced FOXO3A activity.[27] Our data demonstrate that down-regulation of *EGLN2* and accumulation of *FOXO3A* mRNA after DFO treatment is rather consequence of induced hypoxia created by Fe depletion, but neither hypoxia nor *ENGL2*/PHD1-FOXO3A pathway regulate cyclin D1 expression in MCL cells.

Treatment with prolyl hydroxylases inhibitor DMOG decreases MCL cells viability

Despite the fact that direct PHD1 hydroxylase inactivation does not seem to influence regulation of cyclin D1 in MCL, we asked whether inhibition of 2-oxoglutarate-dependent hydroxylases family could have impact on MCL cells viability and cyclin D1 levels. We treated MCL cell lines with prolyl hydroxylase inhibitor (DMOG), a synthetic analog of 2-oxoglutarate which

catalytically inhibits hydroxylation reaction. We found decrease proliferation rate of MCL cells (**Figure 4, upper left panel**), their decreased cyclin D1 protein and mRNA levels while expression of cyclin D1 homologs, *cyclin D2* and *D3* was unchanged (**Figure 4, middle, right panels**). DMOG, similarly to DFO, mimics hypoxia and controls expression of endogenous HIF target genes including down-regulation of the *EGLN2* and up-regulation of the *FOXO3A* mRNA (**Figure 4, lower panels**). Since DMOG is predicted to inhibit broad spectrum of dioxygenases including hydroxylases it is possible that these enzymes have additional substrates with ability to regulate aberrantly expressed *cyclin D1* in MCL cells.

DISCUSSION

In the present study we recapitulated findings that iron chelation is effective in inhibiting proliferation, inducing apoptosis and cell cycle arrest in MCL cell lines and therefore represents a potential non-cytotoxic therapeutic strategy for the treatment of MCL. We also showed that intrinsic overexpression of cyclin D1 makes MCL cells more susceptible to chelation treatment. Future studies will be needed to determine if DFO, or other iron chelators, could be relevant *in vivo* in clinical trials for MCL. We also tested the effect of inhibition of the human 2-oxoglutarate-dependent prolyl hydroxylases on MCL cells. Cells treated with DMOG had decreased proliferation at 24 hours together with down-regulation of cyclin D1 at mRNA and protein level.

Since the role of iron in regulation of *cyclin D1* expression is not completely understood, we investigated the molecular mechanism underlying decreased cyclin D1 mRNA and protein levels in MCL cell lines after DFO-induced iron deficiency. PHDs are dependent on iron[28] to catalyze its hydroxylation activity, thus iron chelation decreases their enzyme activity and increases HIFs. Nevertheless, *EGLN2*/PHD1 LOF in Mino cells did not affect cyclin D1 expression and *FOXO3A* LOF did not restore cyclin D1 levels after chelation treatment. Therefore, the cyclin D1 in MCL cells escapes this regulation circuit and its down-regulation by iron depletion is mediated by another, yet unknown mechanism(s). We hypothesize, that in MCL cells production of cyclin D1, which is aberrantly localized in proximity of a nucleolus and influenced by specific transcription enhancers (e.g. nucleolin)[29] due to t(11;14) translocation, escapes the *ENGL2*/PHD1-FOXO3A regulation.

It is known that iron chelators enhances HIFs-α accumulation[30] and thus induce hypoxia response. We measured expression of *cyclin D1*, *EGLN2* and known HIF target genes *VEGF* and *SLC2A* after 24 hours in 1% O_2 hypoxia and found out that *cyclin D1* level was not altered but *EGLN2* expression was down-regulated suggesting that its down-regulation after DFO treatment is caused by hypoxia. FOXO3A is a transcription factor known to be involved in many cellular processes such as apoptosis[31–33], autophagy[34], oxidative stress[34] and DNA repair.[35] We ruled out the role of FOXO3A in cyclin D1 repression due to iron depletion but we observed accumulation of *FOXO3A* after chelation treatment as a result of induced hypoxia. In many MCL, FOXO3A is constitutively inactivated and its reactivation by nuclear export inhibitors had profound impact on cell viability.[36] We can only speculate that *FOXO3A* induction by chelation treatment would be also beneficial for MCL therapy.

In conclusion, iron chelation and treatment with hydroxylases inhibitor DMOG or by other 2-oxoglutarate-dependent dioxygenase inhibitors decrease MCL cell lines proliferation by down-regulating cyclin D1 mRNA and protein levels. This may be exploited as novel therapeutic avenue. Unlike in other cancer cells, the expression of *cyclin D1* in MCL is not regulated by *EGLN2*/PHD1 nor by FOXO3A and the molecular mechanism controlling cyclin D1 production and degradation in MCL remains to be discovered. Our data indicate that in MCL cells cyclin D1 regulation is not solely driven by *EGLN2*/PHD1, by FOXO3A abundance or by decreased oxygen availability but by intersection of yet to be identified mechanisms which can be targeted by both, 2-oxoglutarate-dependent dioxygenase inhibitors and iron chelators.

ACKNOWLEDGEMENTS

We thanks Heather Gilbert and John Cumming for their effort at the beginning of this project. VD, LL and JTP are supported by Ministry of Education, Youth and Sport, Czech Republic, program INTER-EXCELLENCE, ACTION, LTAUSA17142. Project was supported also from the Ministry of Education, Youth and Sports, Czech Republic, Program NPU I, Project LO1419 (LL, OB, VK). VD is supported by Ministry of Health, project AZV 16-31689A.

CONFLICT OF INTEREST

The authors declare no competing financial interest.

REFERENCES

1. Jares P, Campo E. Advances in the understanding of mantle cell lymphoma. *Br. J. Haematol.* 2008;142(2):149–65.
2. Shah BD, Martin P, Sotomayor EM. Mantle cell lymphoma: a clinically heterogeneous disease in need of tailored approaches. *Cancer Control*. 2012;19(3):227–35.
3. Gilbert H, Cumming J, Prchal JT. Cell Cycle Regulation by Iron: Novel Approaches to Mantle Cell Lymphoma Therapy. *Blood*. 2009;114(22):.
4. Vazana-Barad L, Granot G, Mor-Tzuntz R, et al. Mechanism of the antitumoral activity of deferasirox, an iron chelation agent, on mantle cell lymphoma. *Leuk. Lymphoma*. 2013;54(4):851–9.
5. Robbins E, Pederson T. Iron: its intracellular localization and possible role in cell division. *Proc. Natl. Acad. Sci. U. S. A.* 1970;66(4):1244–51.
6. Hoffbrand A V, Ganeshaguru K, Hooton JW, Tattersall MH. Effect of iron deficiency and desferrioxamine on DNA synthesis in human cells. *Br. J. Haematol.* 1976;33(4):517–26.
7. Nurtjahja-Tjendraputra E, Fu D, Phang JM, Richardson DR. Iron chelation regulates cyclin D1 expression via the proteasome: a link to iron deficiency-mediated growth suppression. *Blood*. 2007;109(9):4045–54.
8. Newman RM, Mobascher A, Mangold U, et al. Antizyme targets cyclin D1 for degradation. A novel mechanism for cell growth repression. *J. Biol. Chem.* 2004;279(40):41504–11.
9. Murakami Y, Hayashi S. Role of antizyme in degradation of ornithine decarboxylase in HTC cells. *Biochem. J.* 1985;226(3):893–6.
10. Murakami Y, Matsufuji S, Kameji T, et al. Ornithine decarboxylase is degraded by the 26S proteasome without ubiquitination. *Nature*. 1992;360(6404):597–599.
11. Asher G, Bercovich Z, Tsvetkov P, Shaul Y, Kahana C. 20S Proteasomal Degradation of Ornithine Decarboxylase Is Regulated by NQO1. *Mol. Cell*. 2005;17(5):645–655.
12. Tsvetkov P, Asher G, Reiss V, et al. Inhibition of NAD(P)H:quinone oxidoreductase 1 activity and induction of p53 degradation by the natural phenolic compound curcumin. *Proc. Natl. Acad. Sci. U. S. A.* 2005;102(15):5535–40.
13. Zhang Q, Gu J, Li L, et al. Control of Cyclin D1 and Breast Tumorigenesis by the EglN2 Prolyl Hydroxylase. *Cancer Cell*. 2009;16(5):413–424.
14. Zheng X, Zhai B, Koivunen P, et al. Prolyl hydroxylation by EglN2 destabilizes FOXO3a by blocking its interaction with the USP9x deubiquitinase. *Genes Dev.* 2014;28(13):1429–1444.
15. Frei C, Edgar BA. Drosophila cyclin D/Cdk4 requires Hif-1 prolyl hydroxylase to drive cell growth. *Dev. Cell*. 2004;6(2):241–51.
16. Metzen E, Berchner-Pfannschmidt U, Stengel P, et al. Intracellular localisation of human HIF-1 alpha hydroxylases: implications for oxygen sensing. *J. Cell Sci.* 2003;116(Pt 7):1319–26.
17. Yasumoto K, Kowata Y, Yoshida A, Torii S, Sogawa K. Role of the intracellular localization of HIF-prolyl hydroxylases. *Biochim. Biophys. Acta - Mol. Cell Res.* 2009;1793(5):792–797.
18. Erez N, Milyavsky M, Goldfinger N, et al. Falkor, a novel cell growth regulator isolated by a functional genetic screen. *Oncogene*. 2002;21(44):6713–6721.
19. Rodriguez J, Herrero A, Li S, et al. PHD3 Regulates p53 Protein Stability by Hydroxylating Proline 359. *Cell Rep.* 2018;24(5):1316–1329.
20. Xie X, Xiao H, Ding F, et al. Over-expression of prolyl hydroxylase-1 blocks NF-κB-mediated cyclin D1 expression and proliferation in lung carcinoma cells. *Cancer Genet.* 2014;207(5):188–194.
21. Scholz CC, Cavadas MAS, Tambuwala MM, et al. Regulation of IL-1β-induced NF-κB by hydroxylases links key hypoxic and inflammatory signaling pathways. *Proc. Natl. Acad. Sci. U. S. A.* 2013;110(46):18490–5.
22. Erez N, Milyavsky M, Eilam R, et al. Expression of prolyl-hydroxylase-1 (PHD1/EGLN2) suppresses hypoxia inducible factor-1alpha activation and inhibits tumor growth. *Cancer Res.* 2003;63(24):8777–83.
23. Takeda K, Aguila HL, Parikh NS, et al. Regulation of adult erythropoiesis by prolyl hydroxylase domain proteins. *Blood*. 2008;111(6):3229–3235.
24. Seth P, Krop I, Porter D, Polyak K. Novel estrogen and tamoxifen induced genes identified by SAGE (Serial Analysis of Gene Expression). *Oncogene*. 2002;21(5):836–843.
25. Klier M, Anastasov N, Hermann A, et al. Specific lentiviral shRNA-mediated knockdown of cyclin D1 in mantle cell lymphoma has minimal effects on cell survival and reveals a regulatory circuit with cyclin D2. *Leukemia*. 2008;22(11):2097–105.

26. Erez N, Stambolsky P, Shats I, et al. Hypoxia-dependent regulation of PHD1: cloning and characterization of the human PHD1/EGLN2 gene promoter. *FEBS Lett.* 2004;567(2–3):311–5.
27. Bakker WJ, Harris IS, Mak TW. FOXO3a is activated in response to hypoxic stress and inhibits HIF1-induced apoptosis via regulation of CITED2. *Mol. Cell*. 2007;28(6):941–53.
28. Tuderman L, Myllylä R, Kivirikko KI. Mechanism of the prolyl hydroxylase reaction. 1. Role of co-substrates. *Eur. J. Biochem.* 1977;80(2):341–8.
29. Allinne J, Pichugin A, Iarovaia O, et al. Perinucleolar relocalization and nucleolin as crucial events in the transcriptional activation of key genes in mantle cell lymphoma. *Blood*. 2014;123(13):2044–53.
30. Woo KJ, Lee T-J, Park J-W, Kwon TK. Desferrioxamine, an iron chelator, enhances HIF-1α accumulation via cyclooxygenase-2 signaling pathway. *Biochem. Biophys. Res. Commun.* 2006;343(1):8–14.
31. Brunet A, Bonni A, Zigmond MJ, et al. Akt promotes cell survival by phosphorylating and inhibiting a Forkhead transcription factor. *Cell*. 1999;96(6):857–68.
32. Stahl M, Dijkers PF, Kops GJPL, et al. The forkhead transcription factor FoxO regulates transcription of p27Kip1 and Bim in response to IL-2. *J. Immunol.* 2002;168(10):5024–31.
33. Ekoff M, Kaufmann T, Engström M, et al. The BH3-only protein Puma plays an essential role in cytokine deprivation induced apoptosis of mast cells. *Blood*. 2007;110(9):3209–17.
34. Nho RS, Hergert P. FoxO3a and disease progression. *World J. Biol. Chem.* 2014;5(3):346.
35. Zhang X, Tang N, Hadden TJ, Rishi AK. Akt, FoxO and regulation of apoptosis. *Biochim. Biophys. Acta - Mol. Cell Res.* 2011;1813(11):1978–1986.
36. Obrador-Hevia A, Serra-Sitjar M, Rodríguez J, Villalonga P, de Mattos SF. The tumour suppressor FOXO3 is a key regulator of mantle cell lymphoma proliferation and survival. *Br. J. Haematol.* 2012;156(3):334–345.

LEGEND TO FIGURE

FIGURE 1

Figure 1. The effect of cellular Fe depletion on human mantle cell lymphoma cell lines (Jeko-1, Mino and HBL-2) and two lymphoma cell lines (SUDHL-6 and DG-75) which do not harbor t(11;14)(q13;32) translocation. All data are represented as the mean of three independent experiments; T bars designate standard deviations; $*P < 0.05$. **A. (Upper panel)** Proliferation rates during DFO (250 μM) treatment in MCL cell lines. Iron chelator DFO inhibited the growth of all MCL cell lines. Cell number and viability were determined using CellometerAutoT4 based on the trypan blue exclusion method. The results are demonstrated as percentage of cell growth in comparison to number of cells at time 0. **(Lower panel)** Percentage of total apoptotic cells (divided into early and late fractions) during DFO treatment. All cell lines exhibited increase in the percentage of apoptotic cells already after 24 hours after Fe depletion but co-incubation of DFO treated cells with Fe source FAC (100 μg/ml) abolished the effect. For detection of apoptotic cells, cell-surface staining was performed with FITC-labeled anti–Annexin V antibody and PI co-staining. **B. (Left panels)** Proliferation rates during DFO treatment (250 μM) in non-MCL cell lines. Iron chelator DFO impaired the growth of non-MCL cell lines but did not inhibit it. Cell number and viability were determined using CellometerAutoT4 based on the trypan blue exclusion method. The results are demonstrated as percentage of cell growth in comparison to number of cells at time 0. **(Right panel)** Percentage of total apoptotic cells (divided into early and late fractions) during DFO treatment. Both lines exhibited increase in the percentage of apoptotic cells after 24-hour treatment. For detection of apoptotic cells, cell-surface staining was performed with FITC-labeled anti–Annexin V antibody and PI co-staining. **C. (Left panel)** Treatment with DFO (250 μM) depleted cyclin D1 protein level. The level of cyclin D1 was not detectable in MCL cell line treated with DFO already after 24 hours. Re-incubation of DFO-treated cells with FAC (100 μg/ml) for 24 hours restores cyclin D1 protein levels. SUDHL-6 and DG-75 cell lines have undetectable level of cyclin D1 (data not shown). **(Right panel)** Cyclin D1 protein level in MCL cell lines after serum-starvation (24 h) and after the release into the medium with 10% FBS or 10% FBS with DFO (250 μM). **D.** Cellular Fe depletion sensitizing MCL cell lines to G1/S arrest. MCL cell lines do not stop cell cycle under serum-starved condition and release with medium containing 10% FBS and DFO (250 μM) sensitizing them to G1/S arrest (comparing to non-MCL cell lines SUDHL-6 and DG-75). Data are demonstrated as percentage of cells in G1 phase. Representative cell cycle histograms analysis by FlowJo software. **E.** Expression analysis of selected genes in DFO-treated (250 μM) MCL cell lines after 24 hours were determined by quantitative PCR. **(Left panel)** Treatment with DFO significantly decreases mRNA expression of *cyclin D1*. **(Middle panel)** The mRNA expression of *cyclin D1* homologs, *cyclin D2 (CD2)* and *cyclin D3 (CD3)*, is not significantly affected by DFO treatment. **(Right panels)** Expression of *EGLN1* gene is significantly increased, the expression of *EGLN2* is significantly decreased and the expression of *EGLN3* is not affected by DFO treatment. In all experiments, data are normalized to *GUSB* and *RPLP0* reference genes.

FIGURE 2

Figure 2. Regulation of cyclin D1 in MCL cell lines is not controlled by *EGLN2*/PHD1 and its hydroxylation target FOXO3A. All data are represented as the mean of three independent experiments; T bars designate standard errors. $*P < 0.05$. Expression analysis are normalized to *GUSB* and/or *RPLP0* reference gene. **A. Loss of *EGLN2*/PHD1 does not affect cellular level of cyclin D1. (Upper left panel)** The decreased expression of *EGLN2* after CRISPR-Cas9 mediated loss-of-function in Mino cell line was determined by quantitative PCR. The expression of *cyclin D1* in these cells did not change. **(Upper right panel)** Parental Mino cell line and *EGLN2*/PHD1 LOF Mino cell line were treated with DFO (250 μM) only or in combination with FAC (100 μg/ml) for 24 hours and protein levels of cyclin D1, PHD1 and CtBP (loading control) were determined by Western blot. **(Lower panel)** The expression analysis of parental Mino cell line and *EGLN2*/PHD1 LOF Mino cell line after DFO (250 μM) and FAC (100 μg/ml) treatment for 24 hours. **B. Loss of FOXO3A does not affect cellular level of *EGLN2*/PHD1 and cyclin D1. (Upper**

left panel) The decreased expression of *FOXO3A* after CRISPR-Cas9 mediated loss-of-function in Mino cell line was determined by quantitative PCR. The expression of *cyclin D1* and *EGLN2* in these cells did not change. **(Upper right panel)** Parental Mino cell line and FOXO3A LOF Mino cell line were treated with DFO (250 μM) only or in combination with FAC (100 μg/ml) for 24 hours and protein levels of FOXO3A, cyclin D1, PHD1 and CtBP (loading control) were determined by Western blot. **(Lower panel)** The expression analysis of parental Mino cell line and FOXO3A LOF Mino cell line after DFO (250 μM) and FAC (100 μg/ml) treatment for 24 hours. **C. FOXO3A up-regulation after DFO (250 μM) treatment.** Treatment with iron chelator for 24 hours increased expression of *FOXO3A* gene in MCL cell lines Jeko-1, Mino and HBL-2.

FIGURE 3

Figure 3. Hypoxia treatment of MCL cell lines. Expression levels of *cyclin D1*, *EGLNs*, selected HIF target genes (*VEGFA* and *SLC2A*) and *FOXO3A* were determined by quantitative PCR after incubation in hypoxia chamber with 1% O_2 for 24 hours. All data are represented as the mean of three independent experiments; T bars designate standard errors. *$P < 0.05$. Expression analyses are normalized to *GUSB* and/or *RPLP0* reference gene. (**Upper panels**) The mRNA expression of HIF target genes (*VEGFA and SLC2A*) are significantly upregulated after DFO and hypoxia treatment. (**Lower panels**) The level of *cyclin D1* was not significantly altered by hypoxia treatment, but we detected down-regulation of *EGLN2* and accumulation of *FOXO3A* mRNA.

FIGURE 4

Figure 4. The effect of PHD inhibitor DMOG (1 mM) on MCL cell lines. (Upper left panel) Proliferation rates during DMOG treatment. Inhibition of PHDs has significant effect on growth of Mino cell line compared to a non-treated control and a control treated with vehicle DMSO (0.2 %, data not shown). Cell number and viability were determined using CellometerAutoT4 based on the trypan blue exclusion method. The results are demonstrated as percentage of cell growth in comparison to the number of cells at time 0. **(Upper middle, right panels)** Treatment with DMOG decreases cellular cyclin D1 level in MCL cell lines. The expression of cyclin D1 was reduced in MCL cell lines after incubation with DMOG for 24 hours on protein and also mRNA level. The mRNA expression of *cyclin D1* homologs, *cyclin D2 (CD2)* and *cyclin D3 (CD3)*, is not significantly affected by DMOG treatment. **(Lower panel)** Expression levels of *EGLNs*, selected HIF target genes (*VEGF* and, *SLC2A*) and *FOXO3A* were determined by quantitative PCR after incubation with DMOG for 24 hours.

FIGURE 1

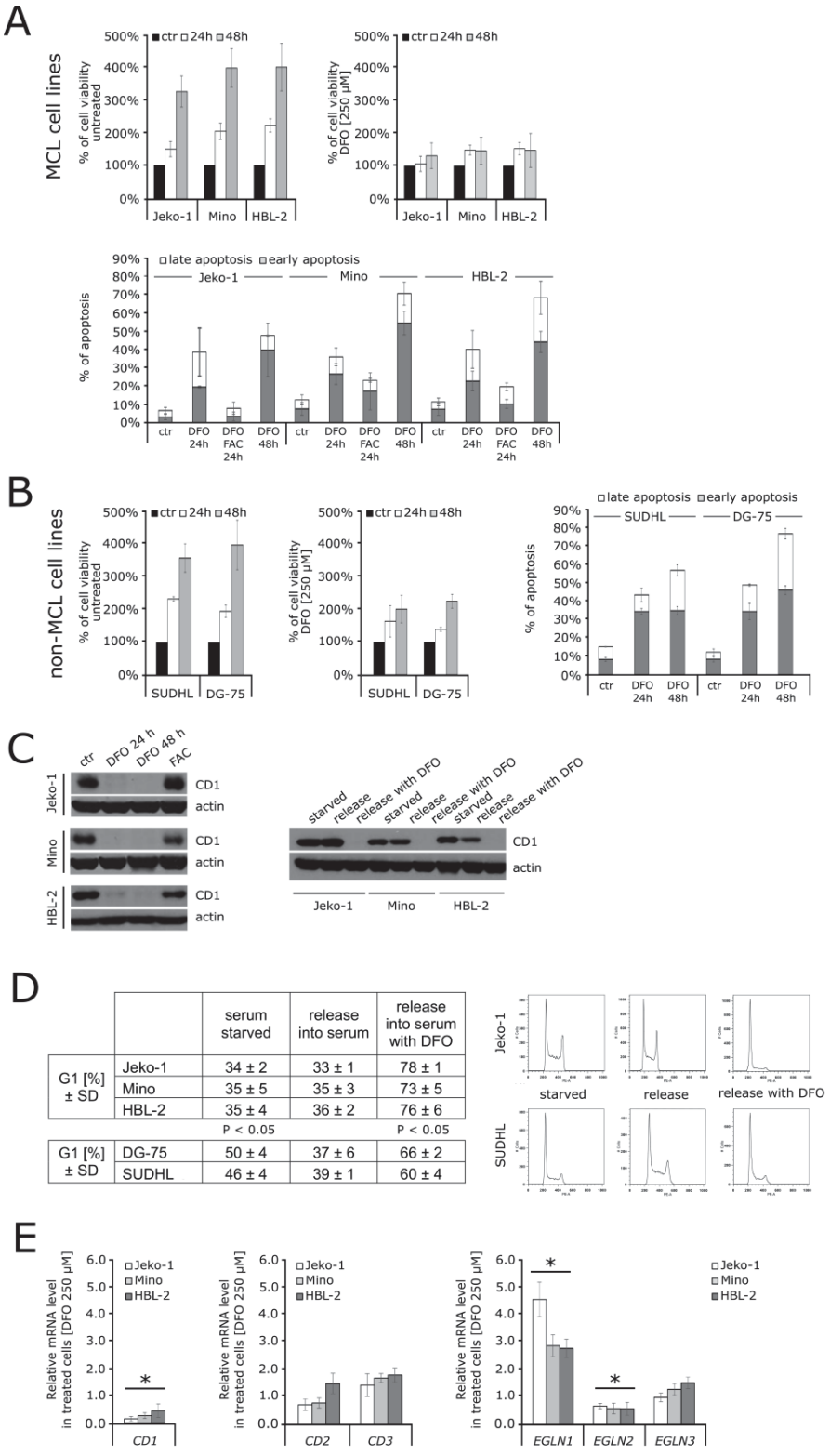
A
MCL cell lines
% of cell viability untreated
% of cell viability DFO [250 µM]
ctr 24h 48h
Jeko-1 Mino HBL-2
% of apoptosis
late apoptosis early apoptosis
ctr DFO 24h DFO FAC 24h DFO 48h
B
non-MCL cell lines
SUDHL DG-75
C
ctr DFO 24 h DFO 48 h FAC
CD1
actin
starved release release with DFO
D
serum starved
release into serum
release into serum with DFO
G1 [%] ± SD
Jeko-1 34 ± 2 33 ± 1 78 ± 1
Mino 35 ± 5 35 ± 3 73 ± 5
HBL-2 35 ± 4 36 ± 2 76 ± 6
P < 0.05 P < 0.05
DG-75 50 ± 4 37 ± 6 66 ± 2
SUDHL 46 ± 4 39 ± 1 60 ± 4
E
Relative mRNA level in treated cells [DFO 250 µM]
CD1 CD2 CD3 EGLN1 EGLN2 EGLN3

FIGURE 2

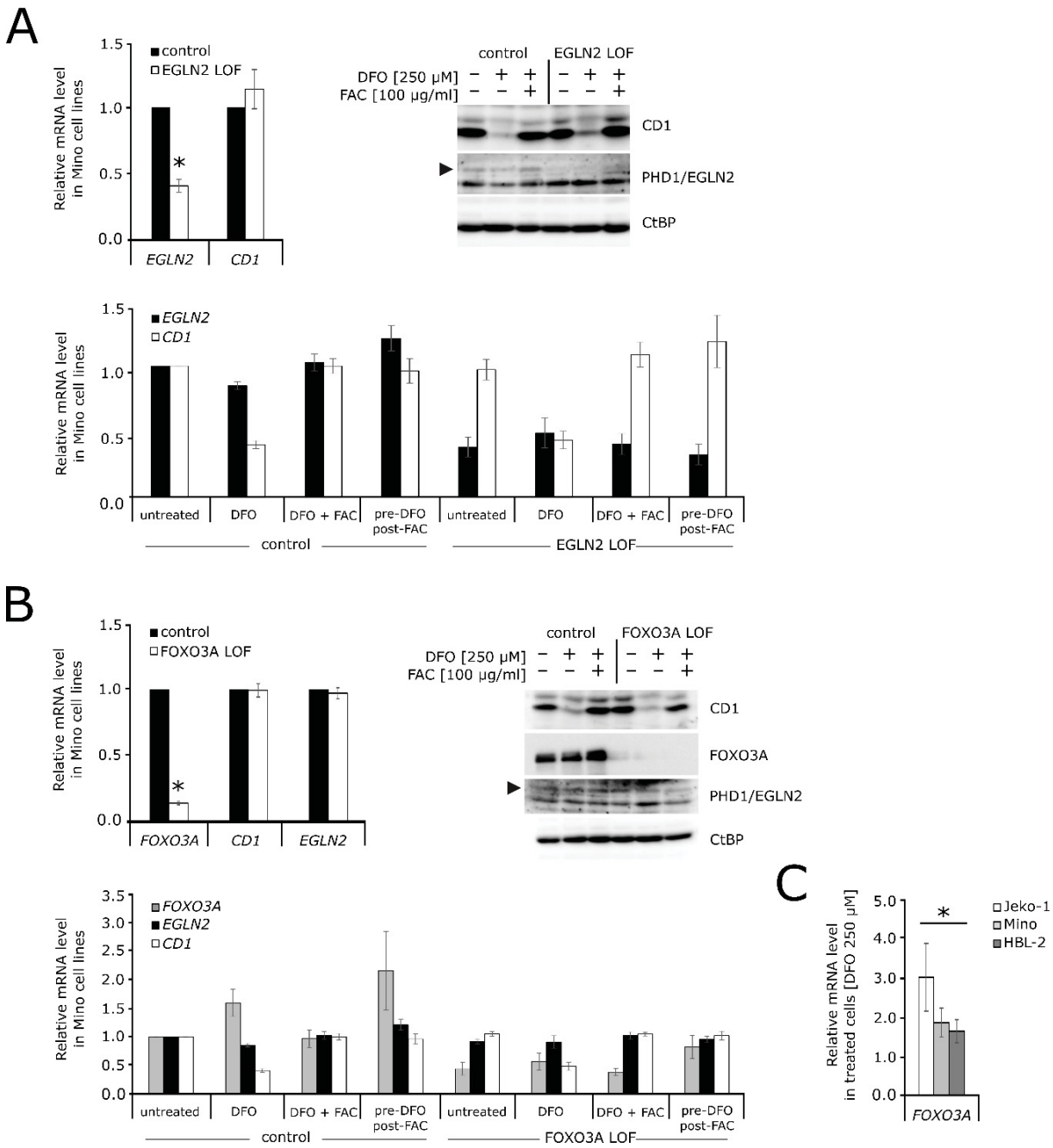
A
control
EGLN2 LOF
Relative mRNA level in Mino cell lines
EGLN2
CD1
DFO [250 µM]
FAC [100 µg/ml]
CD1
PHD1/EGLN2
CtBP
untreated
DFO
DFO + FAC
pre-DFO post-FAC
control
EGLN2 LOF
B
FOXO3A LOF
FOXO3A
C
Jeko-1
Mino
HBL-2
Relative mRNA level in treated cells [DFO 250 µM]

FIGURE 3

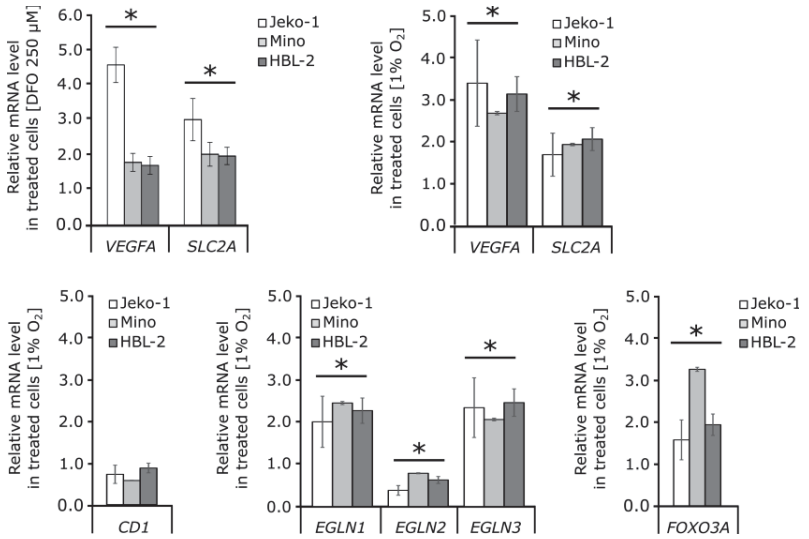
Relative mRNA level in treated cells [DFO 250 µM]
Relative mRNA level in treated cells [1% O2]
Jeko-1
Mino
HBL-2
VEGFA
SLC2A
CD1
EGLN1
EGLN2
EGLN3
FOXO3A
*

FIGURE 4

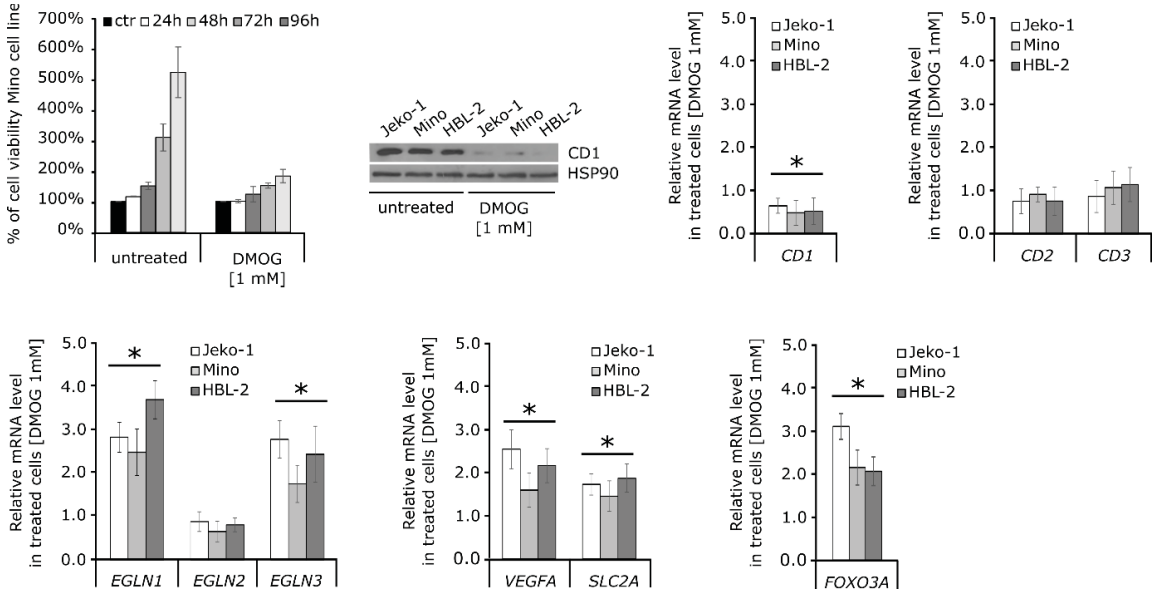
% of cell viability Mino cell line
700%
600%
500%
400%
300%
200%
100%
0%
ctr 24h 48h 72h 96h
untreated
DMOG
[1 mM]
Jeko-1
Mino
HBL-2
Jeko-1
Mino
HBL-2
CD1
HSP90
untreated
DMOG
[1 mM]
Relative mRNA level
in treated cells [DMOG 1mM]
5.0
4.0
3.0
2.0
1.0
0.0
Jeko-1
Mino
HBL-2
*
CD1
Relative mRNA level
in treated cells [DMOG 1mM]
5.0
4.0
3.0
2.0
1.0
0.0
Jeko-1
Mino
HBL-2
CD2
CD3
Relative mRNA level
in treated cells [DMOG 1mM]
5.0
4.0
3.0
2.0
1.0
0.0
Jeko-1
Mino
HBL-2
*
*
EGLN1
EGLN2
EGLN3
Relative mRNA level
in treated cells [DMOG 1mM]
5.0
4.0
3.0
2.0
1.0
0.0
Jeko-1
Mino
HBL-2
*
*
VEGFA
SLC2A
Relative mRNA level
in treated cells [DMOG 1mM]
5.0
4.0
3.0
2.0
1.0
0.0
Jeko-1
Mino
HBL-2
*
FOXO3A